



The combustion kinetics of the lignocellulosic biofuel, ethyl levulinate

Title	The combustion kinetics of the lignocellulosic biofuel, ethyl levulinate
Author(s)	Ghosh, Manik Kumer;Howard, Mícheál Séamus;Zhang, Yingjia;Djebbi, Khalil;Capriolo, Gianluca;Farooq, Aamir;Curran, Henry J.;Dooley, Stephen
Publication Date	2018-04-04
Publisher	Elsevier
Repository DOI	10.1016/j.combustflame.2018.02.028

Manuscript Number: CNF-D-17-00823

Title: The Combustion Kinetics of the Lignocellulosic Biofuel, Ethyl Levulinate

Article Type: Full Length Article

Keywords: Ethyl levulinate, lignocellulosic biofuel, kinetic model, ignition delay, gasoline.

Corresponding Author: Dr. Manik Kumer Ghosh, Ph.D.

Corresponding Author's Institution: Trinity College Dublin

First Author: Manik Kumer Ghosh, Ph.D.

Order of Authors: Manik Kumer Ghosh, Ph.D.; Mícheál S Howard; Yingjia Zhang; Khalil Djebbi; Gianluca Caprilolo; Aamir Farooq, PhD; Curran J Henry, PhD; Dooley Stephen, PhD

Abstract: The combustion kinetics of ethyl levulinate have been investigated. Ethyl levulinate (Ethyl 4-oxopentanoate) is a liquid molecule at ambient temperature, comprising of ketone and ethyl ester functionalities and is one of the prominent liquid fuel candidates that may be easily obtained from lignocellulosic biomass. Shock tube and rapid compression machine apparatuses are utilised to acquire gas phase ignition delay measurements of 0.5% ethyl levulinate/O₂ mixtures at $\phi = 1.0$ and $\phi = 0.5$ at ~ 10 atm over the temperature range 1000–1400 K. Ethyl levulinate is observed not to ignite at temperatures lower than ~ 1040 K in the rapid compression machine. The shock tube and rapid compression machine data are closely consistent and show ethyl levulinate ignition delay to exhibit an Arrhenius dependence to temperature. These measurements are explained by the construction and analysis of a detailed chemical kinetic model. The kinetic model is completed by establishing thermochemical-kinetic analogies to 2-butanone, for the ethyl levulinate ketone functionality, and to ethyl propanoate for the ethyl ester functionality. The so constructed model is observed to describe the shock tube data very accurately, but computes the rapid compression machine data set to a lesser but still applicable fidelity. Analysis of the model suggests the autooxidation mechanism of ethyl levulinate to be entirely dominated by the propensity for the ethyl ester functionality to unimolecularly decompose to form levulinic acid and ethylene. The subsequent reaction kinetics of these species is shown to dictate the overall rate of the global combustion reaction. This model is then used to estimate the Research and Motored Octane Numbers of ethyl levulinate to be ≥ 97.7 and ≥ 93 , respectively. With this analysis ethyl levulinate would be best suited as a gasoline fuel component, rather than with diesel as suggested by the literature. Indeed it may be considered to be useful as an octane booster. The ethyl levulinate kinetic model is constructed within a state-of-the-art gasoline surrogate combustion kinetic model and is thus available as a tool with which to investigate the use of ethyl levulinate as a gasoline additive.

Suggested Reviewers: Joseph W Bozzelli PhD
Professor, Chemistry and Environmental Science, New Jersey Institute
Technology
joseph.w.bozzelli@njit.edu

Zeynep Serinyel PhD
Assistant Professor, Collegium Sciences et Techniques, Université
d'Orleans
zeynep.serinyel@cnrs-orleans.fr

Kieran P Somers PhD
Postdoctoral Research Fellow, Combustion Chemistry Centre, National
University of Galway
kieran.somers@nuigalway.ie

Robert L McCormick PhD
Principal Engineer, U. S. Department of Energy, National Renewable Energy
Laboratory
robert.mccormick@nrel.gov

The Combustion Kinetics of the Lignocellulosic Biofuel, Ethyl Levulinate

Manik Kumer Ghosh^{a,b*}, Mícheál Séamus Howard^{a,b}, Yingjia Zhang^c, Khalil Djebbi^d, Gianluca Capriolo^b, Aamir Farooq^d, Henry J. Curran^c, Stephen Dooley^{a,b*}

^aSchool of Physics, Trinity College Dublin, The University of Dublin, Ireland.

^bDepartment of Chemical Sciences, University of Limerick, Ireland.

^cCombustion Chemistry Centre, National University of Ireland, Galway, Ireland.

^dClean Combustion Research Center, King Abdullah University of Science and Technology, Thuwal, Saudi Arabia.

*Corresponding author:

Manik Kumer Ghosh: ghoshm@tcd.ie

Abstract

The combustion kinetics of ethyl levulinate have been investigated. Ethyl levulinate (Ethyl 4-oxopentanoate) is a liquid molecule at ambient temperature, comprising of ketone and ethyl ester functionalities and is one of the prominent liquid fuel candidates that may be easily obtained from lignocellulosic biomass. Shock tube and rapid compression machine apparatuses are utilised to acquire gas phase ignition delay measurements of 0.5% ethyl levulinate/O₂ mixtures at $\phi = 1.0$ and $\phi = 0.5$ at ~ 10 atm over the temperature range 1000-1400 K. Ethyl levulinate is observed not to ignite at temperatures lower than ~ 1040 K in the rapid compression machine. The shock tube and rapid compression machine data are closely consistent and show ethyl levulinate ignition delay to exhibit an Arrhenius dependence to temperature. These measurements are explained by the construction and analysis of a detailed chemical kinetic model. The kinetic model is completed by establishing thermochemical-kinetic analogies to 2-butanone, for the ethyl levulinate ketone functionality, and to ethyl propanoate for the ethyl ester functionality. The so constructed model is observed to describe the shock tube data very accurately, but computes the rapid compression machine data set to a lesser but still applicable fidelity. Analysis of the model suggests the autooxidation mechanism of ethyl levulinate to be entirely dominated by the propensity for the ethyl ester functionality to unimolecularly decompose to form levulinic acid and ethylene. The subsequent reaction kinetics of these species is shown to dictate the overall rate of the global combustion reaction. This model is then

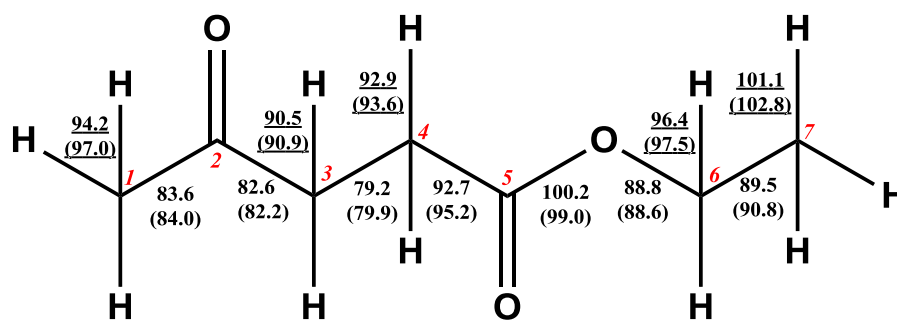
1 use to estimate the Research and Motored Octane Numbers of ethyl levulinate to be ≥ 97.7 and ≥ 93 ,
2 respectively. With this analysis ethyl levulinate would be best suited as a gasoline fuel component,
3 rather than with diesel as suggested by the literature. Indeed it may be considered to be useful as an
4 octane booster. The ethyl levulinate kinetic model is constructed within a state-of-the-art gasoline
5 surrogate combustion kinetic model and is thus available as a tool with which to investigate the use of
6 ethyl levulinate as a gasoline additive.
7
8
9
10
11
12
13
14

15 **Keywords:** Ethyl levulinate, lignocellulosic biofuel, kinetic model, ignition delay, gasoline.
16
17
18
19
20
21
22
23
24
25
26
27
28
29
30
31
32
33
34
35
36
37
38
39
40
41
42
43
44
45
46
47
48
49
50
51
52
53
54
55
56
57
58
59
60
61
62
63
64
65

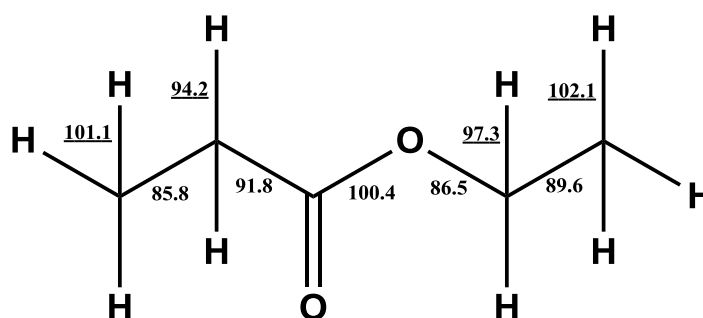
1. Introduction

The catalytic conversion of biomass derived cellulose, hemicellulose and lignin to platform chemicals and fuels has been widely recognised as an opportunity to produce sustainable economies. Ethyl levulinate (EL) (Figure 1) is one of many liquid phase molecules that may be easily produced by the acid hydrolysis of cellulose. It may be produced at the high yields that are essential for potential economic viability, either by reaction of ethanol (the biorefinery platform chemical) and levulinic acid, or by the insitu acid-catalysed reaction of cellulosic sugars with ethanol [1]. The synthetic processes that produce ethyl levulinate from cellulose use ethanol (both as a solvent and reacting partner) as a means of functionalising the levulinic acid precursor [2]. This alkylation also improves the energy density of the cellulose derived functionalities, and their solubility in conventional petroleum derived liquid hydrocarbon fuels. One can also think of the cellulose as improving the fuel properties of Ethanol, notably the energy density. Ethyl levulinate has an energy density of 31.2 MJ/L, much superior to that of ethanol (24 MJ/L). The sustainability benefits of co-reacting cellulose with ethanol are obvious when one realises that 71% of the ethyl levulinate carbon, and 58% of the ethyl levulinate hydrogen are contributed by the cellulose.

Ethyl levulinate



Ethyl propanoate



2-butanone

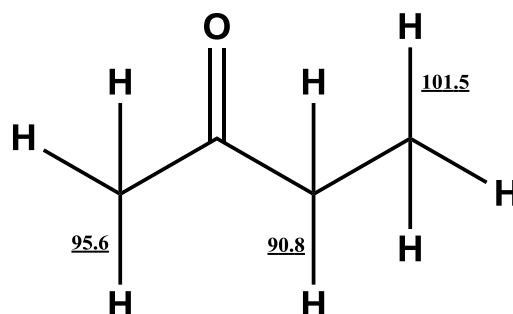


Figure 1. Chemical structures and bond dissociation energies (kcal/mol) of ethyl Levulinate. Carbon-hydrogen bond dissociation energies are underlined. Values without parentheses are average of data produced by isodesmic work reactions calculated at CBS-QB3, CBS APNO and G4MP2 levels of theory [3]. Values in parentheses are group additivity estimates. Ethyl propanoate from [4] and 2-butanone from [5].

Ethyl levulinate (EL) has a high flash point of 90 °C, attributable to its low volatility as prescribed by a boiling point of 206 °C. Due to its high oxygen content ethyl levulinate has been originally espoused as a suitable oxygenate additive for diesel fuels to reduce soot formation. Lei et al. [6], have reported successful engine tests of various blends of ethyl levulinate, and ethyl levulinate/n-butanol with a diesel fuel, showing marginal increases in brake specific fuel consumption and also marginal effect on the emission of unburned hydrocarbons for 10 vol% ethyl levulinate

1 mixtures with a road diesel. Koivistos et al. [7], in a direct injection compression ignition engine,
2 studied a series of oxygenated fuel components both as neat fuels, and as 30 vol% blends with n-
3 heptane. They noted a reduction in overall particulate mass when using ethyl levulinate as a fuel
4 component, but also noted an increase in the overall number of particulate particles. Windom et al. [8]
5 have determined the volatility behaviour of (1–20 vol%) ethyl levulinate blends with Ultra Low
6 Sulphur Diesel (ULSD) and with biodiesel. They show that, while ethyl levulinate is more volatile
7 than either fuel, modest additions of ethyl levulinate to diesel will not significantly affect the overall
8 volatility of the fuel.
9

10
11
12
13
14
15
16
17
18
19
20 The majority of existing literature proposes the use of ethyl levulinate as a sustainable blend-
21 stock for use with diesel fuel, however, the combustion reactivity of ethyl levulinate may present itself
22 as a limiting factor in this regard. Koivistos et al. [7] reported that ethyl levulinate does not ignite at
23 the typical configuration of a tested diesel engine, also noting that ethyl levulinate/n-heptane mixtures
24 showed the longest ignition delays of a large series of fuels tested. Similarly, Murphy et al. [9]
25 corroborate this reactivity indicator when quoting a Derived Cetane Number for ethyl levulinate of “<
26 5”, as deduced by an ignition quality tester. Christensen et al. [10] note that this low cetane number
27 will limit the quantity of ethyl levulinate that might be blended with diesel fuel. The miscibility of
28 ethyl levulinate may also be another constraining factor. Christenson et al. [10] purposely investigated
29 the miscibility of ethyl levulinate with conventional Ultra-Low Sulphur Diesel (ULSD) showing the
30 addition of 10 vol% ethyl levulinate to result in a significantly higher cloud point in comparison to
31 unblended diesel. Moreover, in the range of –10 °C to +10 °C, Christensen et al. [10] report a
32 propensity for a significant fraction of ethyl levulinate to phase separate from the blended diesel. They
33 indicate that this may lead to operational difficulties in vehicle fuel storage tanks and with engine fuel
34 injectors under cold operating conditions. However, both Lake and Burton [11] and Joshi et al. [12]
35 show that such miscibility restrictions are less confining when using biodiesel as the blend
36 component, or as a co-solvent for ethyl levulinate with conventional ultra-low sulphur diesel.
37
38
39
40
41
42
43
44
45
46
47
48
49
50
51
52
53
54
55
56
57
58
59
60
61
62
63
64
65

1 The low cetane number and reactivity of ethyl levulinate may favour its use as a gasoline
2 additive. It is also important to note that ethyl levulinate appears to be more miscible in tested
3
4
5
6
7
8
9
10
11
12
13
14
15
16
17
18
19
20
21
22
23
24
25
26
27
28
29
30
31
32
33
34
35
36
37
38
39
40
41
42
43
44
45
46
47
48
49
50
51
52
53
54
55
56
57
58
59
60
61
62
63
64
65

The low cetane number and reactivity of ethyl levulinate may favour its use as a gasoline additive. It is also important to note that ethyl levulinate appears to be more miscible in tested gasolines than the diesels. Christensen et al. [13] show that at 10 vol% ethyl levulinate did not separate from the gasoline until -40 °C. Christensen et al. [13] also noted that the use of ethyl levulinate (at 3.7 wt% oxygen, ~5.9 mol% ethyl levulinate) as a gasoline extender gives favourable attributes over other possible oxygenated additives, including ethanol and propanols, by; lowering the volatility of the fuel; increasing blended octane numbers by ~15. Similarly, Tian et al. [14] found in both engine and ignition quality tests that ethyl levulinate has a higher anti knock propensity than EURO95 gasoline (RON = 95). This further suggests that ethyl levulinate would be better placed as a gasoline additive. Tian et al., through analogy to ethyl butanoate, espouse that the ethyl levulinate combustion kinetics is dominated by the decomposition pathway to ethylene and levulinic acid, which results in the low reactivity of the molecule. However, a detailed study on the reaction kinetics of ethyl levulinate is needed to test this theory.

The position of the fuel and combustion literature on the prospective uses of ethyl levulinate may thus be summarised as suggesting ethyl levulinate to be intermediate in physical property between gasoline and diesel distillate, but of a kinetic propensity much lower than conventional diesel, and even lower than conventional gasoline. We note that the to-date reactivity indicators are all derived from engine like configurations, where no information of a fundamental kinetic nature is available for reference. This study aims to scientifically resolve the combustion kinetics of ethyl levulinate and their interaction with gasoline combustion kinetics. To achieve this the current study:

- 1) Determines the first entirely gas phase measurements of ethyl levulinate combustion kinetics by the measurement of ignition delay times.

1
2
3
4
5
6
7
8
9
2) Proposes and tests a detailed combustion kinetic model to describe ethyl levulinate and ethyl levulinate/gasoline combustion, and uses this model to make predictions of the octane numbers of ethyl levulinate and ethyl Levulinate/gasoline mixtures.

10 11 12 13 14 15 16 17 18 19 20 21 22 23 24 25 26 27 28 29 30 31 32 33 34 35 36 37 38 39 40 41 42 43 44 45 46 47 48 49 50 51 52 53 54 55 56 57 58 59 60 61 62 63 64 65

Ignition delay times were measured with the Rapid Compression Machine (RCM) Facility at National University of Ireland, Galway and the High Pressure Shock Tube (HPST) facility at King Abdullah University of Science and Technology (KAUST).

The inclusion of three oxygen atoms in the ethyl levulinate molecular structure produces a low vapour pressure of 0.17 mbar at 298 K. The substance is thus difficult to configure gas phase measurements for. As a result, the parameter space of mixture fraction and pressure that the experimental devices of this study can reliably access for the case of ethyl levulinate is constrained. Out of necessity to regulate the ethyl levulinate vapour pressure in the compressed volume of the RCM to be lower than the saturation vapour pressure at the initial operating temperature (348-398 K) of that device by factor of 5, the ethyl levulinate fraction has been restricted to 0.5%, also restricting the compressed pressures safely achievable to ~10 atm. To parameterise the effect of oxygen concentration, ethyl levulinate:oxygen equivalence ratios of 1.0 and 0.5 are selected. For consistency the shock tube examines the same mixture fractions as the RCM study. Experimental details specific to each device follow below.

The twin-opposed piston RCM is a clone of the original NUI Galway (Shell-Thornton) device which produces compression times of approximately 16 ms. Creviced piston heads are used to suppress the formation of vortices within the boundary layer gases, minimizing the effects of temperature inhomogeneities on the intended adiabatic core gas [15]. In this study the narrow range of compressed gas temperatures required to observe the full extent of ethyl levulinate reactivity are achieved by employing a compression ratio of ~ 13:1, N₂/Ar diluent compositions of 65/35 and 40/60

1 mol%, with initial temperatures in the range of 343–393 K. A full accounting of the experimental
2 conditions is provided in Table 1. The ethyl levulinate test fuel (99.85%) is supplied by Sigma-
3 Aldrich Ireland Ltd, while nitrogen (99.95%), oxygen (99.5%) and argon (99.995%) are supplied by
4 BOC Ireland Ltd. Batch mixtures are manometrically prepared in 80 °C mixing tanks twelve hours
5 before conducting experiments.
6
7
8
9

10
11
12
13 The reaction chamber allows for variation of the initial temperature. A gas handling manifold
14 is also heated and its temperatures monitored to keep the reactant mixtures above the saturation
15 temperature of ethyl levulinate at the corresponding compressed pressure at all times. The pressure
16 history inside the reaction chamber is measured using a pressure transducer (Kistler 603B) and a
17 charge amplifier (Kistler 5018). Both the pressure and piston position signals are recorded by a digital
18 oscilloscope (PicoScope 4424). The non-linearity of the pressure transducer is less than ±1% of the
19 full scale output. The compression pressure was held at 10 atm to within 3% for all of the experiments
20 presented, see Table 1. A photomultiplier detector (Hamamastu 166) was used to record the emission
21 of light and the measured ignition delay times are reproducible to ±15%.
22
23
24
25
26
27
28
29
30
31
32

33
34
35 As the RCM environment is characterised by heat losses [15], the compressed temperature is
36 determined from the measurement of the compressed pressure by the isentropic relationship;
37
38
$$\ln\left(\frac{p_c}{p_i}\right) = \int_{T_i}^{T_c} \frac{\gamma}{\gamma-1} \frac{dT}{T}$$
, where γ is the compressibility of the test gas; the compressed pressure, p_c ; the
39 initial pressure, p_i ; the compressed temperature, T_c ; and the initial temperature; T_i . Non-reactive
40 experiments are performed to account for the dynamic effect of heat losses, allowing the temperature
41 history experienced to be approximated in zero dimensional simulations of the RCM ignition
42 experiments. The non-reactive measurements replace oxygen with the inert, nitrogen, which has a
43 similar compressibility value of γ . Typical reactive and accompanying non-reactive pressure and
44 emission histories are shown in Figure 2. Considering the weak ignition energy release events
45
46
47
48
49
50
51
52
53
54
55
56
57
58
59
60
61
62
63
64
65

(discussed below) for these dilute mixtures, the ignition delay time was defined as the time from the end of compression to the subsequent peak of light emission, see Figure 2.

The experimental uncertainty is ± 10 K in reported temperatures, ± 0.1 atm in reported pressures, $\pm 15\%$ in reported ignition delay times and $< 1\%$ (relative) in reported mixture fractions.

Initial Pressure / atm	Initial Temperature / K	Compressed Pressure / atm	Compressed Temperature / K	Ignition Delay Time / ms
EL/O ₂ /N ₂ /Ar, 0.005/0.0425/0.6185/0.334 ϕ 1.0				
*0.240	348	10.16	1130	2.00
*0.240	348	10.14	1129	1.98
0.264	388	9.79	1098	8.55
0.264	388	9.79	1098	8.16
0.264	388	9.81	1099	7.15
0.266	393	10.00	1115	5.24
0.266	393	9.90	1112	4.32
0.264	383	9.77	1085	14.51
0.264	383	9.74	1084	16.09
0.264	373	9.96	1065	34.57
0.264	373	9.92	1064	39.34
EL/O ₂ /N ₂ /Ar, 0.005/0.085/0.546/0.364 ϕ 0.5				
0.264	373	9.93	1073	8.36
0.264	373	10.25	1078	8.79
0.264	373	10.29	1079	9.52
0.264	383	10.04	1097	2.98
0.264	383	10.17	1101	3.15
0.264	383	10.20	1102	2.78
0.264	393	10.00	1121	0.98
0.264	393	10.29	1130	1.10
0.264	393	10.22	1128	1.43
0.257	363	9.70	1048	39.21
0.257	363	9.79	1051	35.91

Table 1. Rapid compression machine initial and compressed conditions, and ignition delay times.

*Mixture composition is EL/O₂/N₂/Ar, 0.005/0.0425/0.381/0.5715.

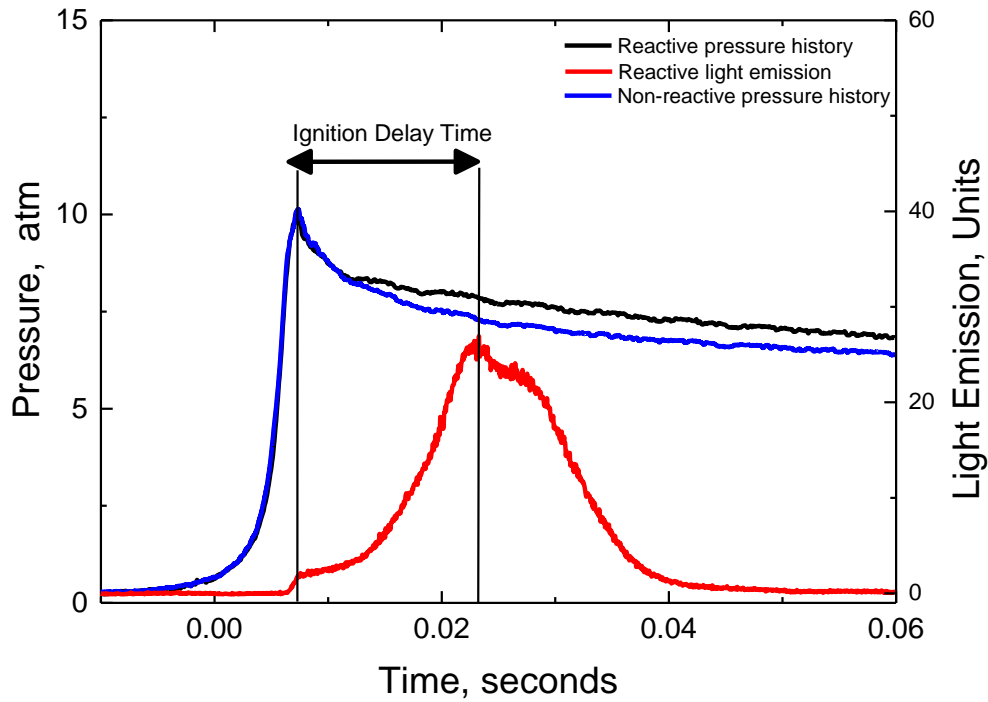


Figure 2. Exemplar rapid compression machine experimental (pressure and light) histories for compressed conditions of 9.74 atm and 1084 K, EL/O₂/N₂/Ar, 0.005/0.0425/0.6185/0.334, $\phi = 1.0$.

The experimental configuration of the high pressure shock tube (HPST) facility at KAUST has been detailed elsewhere [16]. The stainless steel HPST with inner diameter of 10 cm, driven section of 6.6 m and a driver section that can be varied in length to 6.6 m. For these intended 10 bar reflected shock pressures, the driver and driven sections are separated by a mid-section which holds two pre-scored 0.13 mm aluminium diaphragms. Five equally separated PCB 113B26 piezoelectric pressure transducers (PZT) are placed axially in the last 1.5 m of the driven section to measure incident shock velocity. The pressure history inside the shock tube is recorded using a Kistler 603B1 piezoelectric transducer located 1 cm away from the end-wall. OH* chemiluminescence at 306 nm is monitored using a modified photodetector (Thorlabs PDA36A) through a sapphire window at the side-wall.

Two stainless steel mixing vessels attached to the driven section are used to prepare gaseous EL/O₂/Ar mixtures. The driven section of the shock tube, the mixing vessels and the connecting tubes

1 are heated to 110 °C to avoid condensation of ethyl levulinate. Ethyl levulinate is injected into the
2 evacuated and heated (110 °C) stainless steel mixing vessels with its partial pressure kept at two-
3 thirds or less of the saturation vapor pressure. Oxygen (99.999%) and argon (99.999%) are
4 manometrically mixed with the fuel in the mixing. A magnetically driven stirrer is used for at least
5 one hour to produce homogeneous mixtures.
6
7
8
9

10
11
12
13 The driver section is pressurized with helium and the mid-section with helium at half the
14 pressure of the driver section. The shock wave is then initiated by venting the mid-section, causing the
15 diaphragms to rupture due to the resulting pressure gradient. This procedure is repeated at various
16 gradients to induce a range of shock velocities producing the reflected shock conditions and ignition
17 delay times given in Table 2.
18
19
20
21
22
23
24
25

26
27 In the shock tube study, the ignition delay time is defined as the time from the arrival of the
28 reflected shock wave at the side-wall to the subsequent maximum rate of change of pressure or OH*
29 emission. Ignition delay times calculated using the pressure and OH* signal generally differed by less
30 than 3%. However, due to the dilute mixtures used here, the pressure increase at ignition was
31 relatively small at the lower temperatures studied and the OH* signal provides for a more precise
32 determination of the onset of ignition. A representative ignition delay time measurement is shown in
33 Figure 3. The experimental uncertainty is $\pm 0.7\%$ in reported temperatures, $\pm 1\%$ in reported pressures,
34 $\pm 20\%$ in reported ignition delay times and $\pm 2\%$ in reported mixture fractions.
35
36
37
38
39
40
41
42
43
44
45
46
47
48
49
50
51
52
53
54
55
56
57
58
59
60
61
62
63
64
65

Pressure / bar	Temperature / K	Ignition Delay Time / ms
EL/O ₂ /Ar, 0.005/0.0425/0.9525, ϕ 1.0		
9.1	1391	0.070
10.4	1352	0.164
10.3	1311	0.293
10.4	1274	0.418
10.4	1250	0.577
10.5	1204	1.057
EL/O ₂ /Ar, 0.005/0.085/0.91, ϕ 0.5		
10.6	1340	0.117
10.4	1324	0.146
10.4	1250	0.426
9.7	1236	0.507
10.2	1213	0.693
10.3	1185	1.014
9.9	1150	1.590
9.8	1131	2.213
9.9	1125	2.702
10.0	1116	2.610

Table 2. Shock tube compressed conditions and ignition delays times.

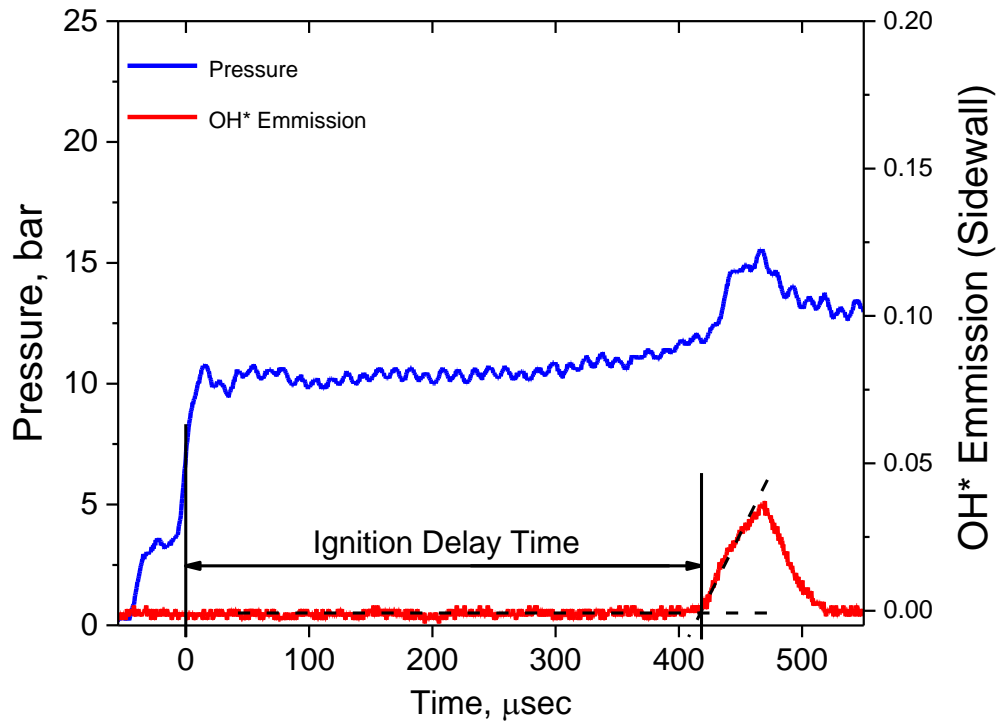


Figure 3. Exemplar shock tube experimental (pressure and light) histories for compressed conditions of 10.4 bar and 1250 K, EL/O₂/Ar, 0.005/0.085/0.91, ϕ =0.5.

3. Computational Methods

1 For oxygenated hydrocarbons bearing the ethyl ester or methyl ketone functionalities, reliable
2 thermochemical quantities already exist [4, 5], and are most conveniently utilised in the context of
3 chemical group additivity. To estimate ethyl levulinate thermochemistry, one can use the
4 thermochemistry of 2-butanone as methyl ketone (atoms 1–3 in Figure 1) and ethyl propanoate as
5 ethyl ester (atoms 4–7 in Figure 1) functionalities respectively. However, the thermochemical
6 properties of the methylene groups located between the ethyl-ester and methyl-ketone moieties of
7 ethyl levulinate present unstudied identities within the context of combustion kinetics. Consequently,
8 it is expected that existing thermochemical group contributions available to estimate radical formation
9 enthalpies associated with these identities are inappropriate.
10
11
12
13
14
15
16
17
18
19
20
21
22
23

24 Therefore, a complete set of molecule and radical formation enthalpies for the ethyl levulinate
25 pyrolysis system are pursued by computational chemistry methods [3]. When combined with well-
26 known reference values for small radicals, this data also produces reliable estimates of the bond
27 dissociation energies of ethyl levulinate that are essential components of the kinetic model,
28 particularly in the assignment of hydrogen abstraction rate constants. The computational chemistry
29 methods give chemically accurate values and it involves several different levels of theory (i.e. CBS-
30 QB3, CBS-APNO, and G4MP2), the findings are summarised in Table 3 [3]. A detailed description
31 of those findings is too large to be included in the scope of the current contribution and is reported
32 separately, and available from the authors upon request [3].
33
34
35
36
37
38
39
40
41
42
43
44
45
46
47
48
49
50
51
52
53
54
55
56
57
58
59
60
61
62
63
64
65

Species	Average (CBS-QB3 + CBS-APNO + G4MP2)
<i>Molecules</i>	
CH ₃ C(O)CH ₂ CH ₂ C(O)OCH ₂ CH ₃	-148.1
CH ₃ C(O)CH ₂ CH ₂ C(O)OH	-145.3
CH ₃ C(O)CH ₂ CH ₂ C(O)OCH ₃	-140.0
<i>Alkyl and Alkoxy Radicals Derived From Ethyl Levulinate C–C and C–O Fission</i>	
CH ₃ C(O)CH ₂ CH ₂ Ċ(O)	-45.0
CH ₃ C(O)CH ₂ CH ₂ C(O)Ġ	-88.0
CH ₃ C(O)CH ₂ CH ₂ C(O)OĊH ₂	-93.7
Ċ(O)CH ₂ CH ₂ C(O)OCH ₂ CH ₃	-99.6
<i>Alkyl Radicals Derived From Ethyl Levulinate C–H Fission</i>	
ĊH ₂ C(O)CH ₂ CH ₂ C(O)OCH ₂ CH ₃	-106.0
CH ₃ C(O)ĊHCH ₂ C(O)OCH ₂ CH ₃	-109.8
CH ₃ C(O)CH ₂ ĊHC(O)OCH ₂ CH ₃	-107.3
CH ₃ C(O)CH ₂ CH ₂ C(O)OĊHCH ₃	-103.8
CH ₃ C(O)CH ₂ CH ₂ C(O)OCH ₂ ĊH ₂	-99.1

Table 3: Computed enthalpies of formation, ΔH_f^0 (298.15 K) (kcal/mol) for radicals and molecules of the ethyl levulinate oxidation system employingisodesmic work reactions [3].

4. Combustion Kinetic Model Construction

From a discrete molecular perspective, the combustion kinetics of levulinate ester chemical structures have not been studied before. The ethyl levulinate structure is markedly different to conventional paraffinic hydrocarbons, and other oxygenates as it bares both ketone, and ethyl ester functionalities in the same molecule. However, from the perspective of functional groups, both the methyl ketone, and ethyl ester moieties are quite well studied. Thus, having established the thermochemical environments of the species of the ethyl levulinate oxidation mechanism, the elementary reaction pathways, their rate constant expressions pertinent to ethyl levulinate combustion can be prescribed considering the best knowledge available for each discrete reaction center, as studied in these other, simpler systems. In general, for the ethyl levulinate reaction centers comprising the methyl ketone functionality (atoms 1–3 in Figure 1), rate constant parameters have been assigned by analogy to those of 2-butanone, and for those reaction centers comprising the ethyl ester

1
2
3
4
5
6
7
8
9
10
11
12
13
14
15
16
17
18
19
20
21
22
23
24
25
26
27
28
29
30
31
32
33
34
35
36
37
38
39
40
41
42
43
44
45
46
47
48
49
50
51
52
53
54
55
56
57
58
59
60
61
62
63
64
65

functionality (atoms 4–7 in Figure 1), rate constant parameters have been assigned by analogy to those of the well-studied ethyl propanoate system. These are assigned principally by considering the modelling works of Serinyel et al. [17] and Metcalfe and co-workers [18, 19], for the methyl ketone and ethyl ester functionalities respectively. The appropriateness of the analogies imposed above is supported by a similarity in the thermochemical environment local to each reaction center as has been described above to within an apparent worst case consistency of 3.1 kcal/mol.

The thermochemistry of all species produced by homolytic cleavage of ethyl levulinate, and their consumption products that are not described in the reaction submodel have been estimated by group additivity employing THERM [20]. The ketone group contributions are adopted from those reported by Hudzik et al. [5], and the ethyl ester contributions consistent with the finding of El-Nahas et al. [4] for the case of ethyl propanoate. These calculations result in a set of bond dissociation energies for ethyl levulinate, as shown by Figure 1. The formation enthalpy from these group additivity estimates is then adjusted to be equal to the theoretically calculated value we recommend in Table 3 above.

Reaction pathways have been prescribed by precise analogy to the descriptors used for the analogous reaction centers of 2-butanone and ethyl propanoate. Temperature dependent reaction rate constants are defined in the model with use of the modified Arrhenius equation, $k = A T^n \exp(-E_a/RT)$ where, the frequency factor, A; the temperature, T; the activation energy, E_a ; and the Universal Gas Constant, R. As is the norm in the field, this paper uses units of $\text{cm}^3 \text{mole}^{-1} \text{s}^{-1}$, K and calories. In all cases, reactions are prescribed to be microscopically reversible, generally according to the protocols of Curran et al. [21, 22] e.g., where radical decomposition rate constants are estimated in the reverse exothermic direction ($P+Q \Rightarrow R$) allowing the forward ($R \Rightarrow P+Q$) rate constant to be calculated from the equilibrium constant. The acquisition of accurate thermochemical parameters outlined above is essential to the fidelity of the rate constants estimated by this methodology.

1
2
3
4
5
6
7
8
9
10
11
12
13
14
15
16
17
18
19
20
21
22
23
24
25
26
27
28
29
30
31
32
33
34
35
36
37
38
39
40
41
42
43
44
45
46
47
48
49
50
51
52
53
54
55
56
57
58
59
60
61
62
63
64
65

Importantly, the gas phase reaction of ethyl esters has been repeatedly observed to be characterised by the concerted elimination of the ethyl group to form ethylene and the corresponding acid. For example, see the works of Blades and Gilderson [23], and Metcalfe et al. [18, 19], showing ethyl propanoate to decompose to ethylene and propanoic acid, and Westbrook et al. [24], who show the formation of formic acid and ethylene from ethyl formate decomposition. These findings are further evidenced by the works of Farooq et al. [25] who studied ethyl propanoate pyrolysis, and by the work of Ren et al. [26] who studied the thermal decomposition of a series of ethyl esters behind reflected shock waves. In all cases, the particular ethyl ester was concluded to eliminate to the acid and ethylene as the dominant process. Metcalfe et al. [19] refined the high pressure limit rate expression for the reaction ethyl propanoate \rightleftharpoons propanoic acid + ethylene to $1.6 \times 10^{13} \times \text{Exp} \left(\frac{50,000 \text{ cal/mol}}{RT} \right) \text{ s}^{-1}$. Westbrook had similarly found a rate expressions of $2.0 \times 10^{13} \times \text{Exp} \left(\frac{50,000 \text{ cal/mol}}{RT} \right)$ and $1.0 \times 10^{13} \times T^{0.0} \times \text{Exp} \left(\frac{50,000 \text{ cal/mol}}{RT} \right)$ to adequately describe the similar processes of ethyl acetate and ethyl formate respectively. An activation energy of 50.2 kcal/mol for ethyl levulinate elimination to levulinic acid and ethylene is also computed from theory [3]. As this is very similar to the $1.6 \times 10^{13} \times T^{0.0} \times \text{Exp} \left(\frac{50,000 \text{ cal/mol}}{RT} \right) \text{ s}^{-1}$ rate expression tested by Metcalfe et al. for ethyl propanoate, this rate expression is assigned to the reaction of ethyl levulinate \rightleftharpoons levulinic acid and ethylene.

4.1 Hydrogen Abstraction from Ethyl Levulinate

From Figure 1 and Table 3, it is established that ethyl levulinate has a remarkable variety of weak covalent bonds. This is particularly the case with regard to its C–H bonds, four out of the five of these are weaker than or equal to ~ 96 kcal/mol, the typical energy of a tertiary C–H bond in paraffinic systems. This C–H bonding environment is therefore a significant departure from the combustion kinetics experience base. In the present model, hydrogen abstraction from carbon atoms 1, 3, 4 and 6 (90.5–96.4 kcal/mol, Figure 1) have been prescribed reaction rate coefficients, on a per hydrogen atom basis, equivalent to those utilised for hydrogen abstraction from tertiary carbon atoms [27, 28]. The importance of this assignment is discussed when analysing the kinetic model calculations.

1
2 *4.2 Levulinic Acid Submodel*
3

4 Levulinic acid is a major intermediate species in the combustion of ethyl levulinate. The
5 thermochemistry of this molecule is analogous to that of ethyl levulinate with the exception of the
6 acidic C–H bond, which is expected to have a bond dissociation energy of ~ 110 kcal/mol. The
7 hydrogen abstraction rate constants for this molecule have been assigned consistent with the
8 prescription above to ethyl levulinate, with the acidic site being assumed as equivalent to a primary
9 hydrogen atom. The entire ethyl levulinate and levulinic acid submodels are listed in Table 4.
10
11
12
13
14
15
16
17
18
19
20
21
22
23
24
25
26
27
28
29
30
31
32
33
34
35
36
37
38
39
40
41
42
43
44
45
46
47
48
49
50
51
52
53
54
55
56
57
58
59
60
61
62
63
64
65

Reaction	A	n	E _a	Reference
<i>Ethyl Levulinate Decomposition</i>				
EL1J + \dot{H} + M \rightleftharpoons EL	1 x 10 ¹⁴	0.00	0.0	High pressure limit, analogy to ethyl propanoate [18, 19].
EL3J + \dot{H} + M \rightleftharpoons EL	1 x 10 ¹⁴	0.00	0.0	High pressure limit, analogy to ethyl propanoate [18, 19].
EL4J + \dot{H} + M \rightleftharpoons EL	1 x 10 ¹⁴	0.00	0.0	High pressure limit, analogy to ethyl propanoate [18, 19].
EL6J + \dot{H} + M \rightleftharpoons EL	1 x 10 ¹⁴	0.00	0.0	High pressure limit, analogy to ethyl propanoate [18, 19].
EL7J + \dot{H} + M \rightleftharpoons EL	1 x 10 ¹⁴	0.00	0.0	High pressure limit, analogy to ethyl propanoate [18, 19].
$\dot{C}H_3 + \dot{C}(O)CH_2CH_2C(O)OCH_2CH_3 \rightleftharpoons EL$	3 x 10 ¹³	0.00	0.0	High pressure limit, analogy to ethyl propanoate [18, 19].
$CH_3C(O)CH_2\dot{C}H_2 + \dot{C}(O)OCH_2CH_3 \rightleftharpoons EL$	3 x 10 ¹³	0.00	0.0	High pressure limit, analogy to ethyl propanoate [18, 19].
$CH_3C(O)CH_2CH_2\dot{C}(O) + C_2H_5\dot{O} \rightleftharpoons EL$	3 x 10 ¹³	0.00	0.0	High pressure limit, analogy to ethyl propanoate [18, 19].
$CH_3C(O)CH_2CH_2\dot{C}O_2 + \dot{C}_2H_5 \rightleftharpoons EL$	3 x 10 ¹³	0.00	0.0	High pressure limit, analogy to ethyl propanoate [18, 19].
$EL \rightleftharpoons CH_3C(O)CH_2\dot{C}H_2C(O)OH + C_2H_4$	8 x 10 ¹²	0.00	49,950	See detailed description in text.
<i>Hydrogen Abstraction from Ethyl Levulinate by H atom</i>				
EL + $\dot{H} \rightleftharpoons EL1J + H_2$	1.81 x 10 ⁶	2.40	2,583	Assumed to be 3 x hydrogen abstraction from tertiary carbon [27].
EL + $\dot{H} \rightleftharpoons EL3J + H_2$	1.20 x 10 ⁶	2.40	2,583	Assumed to be 2 x hydrogen abstraction from tertiary carbon [27].
EL + $\dot{H} \rightleftharpoons EL4J + H_2$	1.20 x 10 ⁶	2.40	2,583	Assumed to be 2 x hydrogen abstraction from tertiary carbon [27].
EL + $\dot{H} \rightleftharpoons EL6J + H_2$	1.20 x 10 ⁶	2.40	2,583	Assumed to be 2 x hydrogen abstraction from tertiary carbon [27].
EL + $\dot{H} \rightleftharpoons EL7J + H_2$	6.03 x 10 ⁵	2.54	6,756	Assumed to be 3 x hydrogen abstraction from primary carbon [27].
<i>Hydrogen Abstraction from Ethyl Levulinate by Hydroxyl Radical</i>				
EL + $\dot{O}H \rightleftharpoons EL1J + H_2O$	8.78 x 10 ⁴	2.53	-1,659	Assumed to be 3 x hydrogen abstraction from tertiary carbon [27].
EL + $\dot{O}H \rightleftharpoons EL3J + H_2O$	5.85 x 10 ⁴	2.53	-1,659	Assumed to be 2 x hydrogen abstraction from tertiary carbon [27].
EL + $\dot{O}H \rightleftharpoons EL4J + H_2O$	5.85 x 10 ⁴	2.53	-1,659	Assumed to be 2 x hydrogen abstraction from tertiary carbon [27].
EL + $\dot{O}H \rightleftharpoons EL6J + H_2O$	5.85 x 10 ⁴	2.53	-1,659	Assumed to be 2 x hydrogen abstraction from tertiary carbon [27].
EL + $\dot{O}H \rightleftharpoons EL7J + H_2O$	2.22 x 10 ⁴	2.67	-168.9	Assumed to be 3 x hydrogen abstraction from primary carbon [27].
<i>Hydrogen Abstraction from Ethyl Levulinate by Methyl Radical</i>				
EL + $\dot{C}H_3 \rightleftharpoons EL1J + CH_4$	2.71	3.46	4598	Assumed to be 3 x hydrogen abstraction from tertiary carbon [27].
EL + $\dot{C}H_3 \rightleftharpoons EL3J + CH_4$	1.81	3.46	4598	Assumed to be 2 x hydrogen abstraction from tertiary carbon [27].
EL + $\dot{C}H_3 \rightleftharpoons EL4J + CH_4$	1.81	6.36	893	Assumed to be 2 x hydrogen abstraction from tertiary carbon [27].
EL + $\dot{C}H_3 \rightleftharpoons EL6J + CH_4$	1.81	6.36	893	Assumed to be 2 x hydrogen abstraction from tertiary carbon [27].
EL + $\dot{C}H_3 \rightleftharpoons EL7J + CH_4$	4.53 x 10 ⁻¹	3.65	7,154	Assumed to be 3 x hydrogen abstraction from primary carbon [27].
<i>Hydrogen Abstraction from Ethyl Levulinate by Methoxy Radical</i>				
EL + $CH_3\dot{O} \rightleftharpoons EL1J + CH_3OH$	5.70 x 10 ¹⁰	0.00	2,800	Assumed to be 3 x hydrogen abstraction from tertiary carbon [27].
EL + $CH_3\dot{O} \rightleftharpoons EL3J + CH_3OH$	3.80 x 10 ¹⁰	0.00	2,800	Assumed to be 2 x hydrogen abstraction from tertiary carbon [27].
EL + $CH_3\dot{O} \rightleftharpoons EL4J + CH_3OH$	3.80 x 10 ¹⁰	0.00	2,800	Assumed to be 2 x hydrogen abstraction from tertiary carbon [27].
EL + $CH_3\dot{O} \rightleftharpoons EL6J + CH_3OH$	3.80 x 10 ¹⁰	0.00	2,800	Assumed to be 2 x hydrogen abstraction from tertiary carbon [27].
EL + $CH_3\dot{O} \rightleftharpoons EL7J + CH_3OH$	1.60 x 10 ¹¹	0.00	7,000	Assumed to be 3 x hydrogen abstraction from primary carbon [27].
<i>Hydrogen Abstraction from Ethyl Levulinate by Ethoxy Radical</i>				

6	$\text{EL} + \text{CH}_3\dot{\text{O}}_2 \rightleftharpoons \text{EL1J} + \text{CH}_3\text{O}_2\text{H}$	4.10×10^{-2}	3.12	13,190	Assumed to be 3 x hydrogen abstraction from tertiary carbon [27].
7	$\text{EL} + \text{CH}_3\dot{\text{O}}_2 \rightleftharpoons \text{EL3J} + \text{CH}_3\text{O}_2\text{H}$	2.73×10^{-2}	3.12	13,190	Assumed to be 2 x hydrogen abstraction from tertiary carbon [27].
8	$\text{EL} + \text{CH}_3\dot{\text{O}}_2 \rightleftharpoons \text{EL4J} + \text{CH}_3\text{O}_2\text{H}$	2.73×10^{-2}	3.12	13,190	Assumed to be 2 x hydrogen abstraction from tertiary carbon [27].
9	$\text{EL} + \text{CH}_3\dot{\text{O}}_2 \rightleftharpoons \text{EL6J} + \text{CH}_3\text{O}_2\text{H}$	2.73×10^{-2}	3.12	13,190	Assumed to be 2 x hydrogen abstraction from tertiary carbon [27].
10	$\text{EL} + \text{CH}_3\dot{\text{O}}_2 \rightleftharpoons \text{EL7J} + \text{CH}_3\text{O}_2\text{H}$	6.93×10^{-1}	3.97	18,280	Assumed to be 3 x hydrogen abstraction from primary carbon [27].
<i>Hydrogen Abstraction from Ethyl Levulinate by Hydroxyl Radical</i>					
12	$\text{EL} + \text{H}\dot{\text{O}}_2 \rightleftharpoons \text{EL1J} + \text{H}_2\text{O}_2$	1.30×10^{-3}	3.01	12,090	Assumed to be 3 x hydrogen abstraction from tertiary carbon [27].
13	$\text{EL} + \text{H}\dot{\text{O}}_2 \rightleftharpoons \text{EL3J} + \text{H}_2\text{O}_2$	8.66×10^{-2}	3.01	12,090	Assumed to be 2 x hydrogen abstraction from tertiary carbon [27].
14	$\text{EL} + \text{H}\dot{\text{O}}_2 \rightleftharpoons \text{EL4J} + \text{H}_2\text{O}_2$	8.66×10^{-2}	3.01	12,090	Assumed to be 2 x hydrogen abstraction from tertiary carbon [27].
15	$\text{EL} + \text{H}\dot{\text{O}}_2 \rightleftharpoons \text{EL6J} + \text{H}_2\text{O}_2$	8.66×10^{-2}	3.01	12,090	Assumed to be 2 x hydrogen abstraction from tertiary carbon [27].
16	$\text{EL} + \text{H}\dot{\text{O}}_2 \rightleftharpoons \text{EL7J} + \text{H}_2\text{O}_2$	2.04×10^{-1}	3.59	17,160	Assumed to be 3 x hydrogen abstraction from primary carbon [27].
<i>Hydrogen Abstraction from Ethyl Levulinate by O atom</i>					
18	$\text{EL} + \ddot{\text{O}} \rightleftharpoons \text{EL1J} + \dot{\text{O}}\text{H}$	5.90×10^{-5}	2.40	1,150	Assumed to be 3 x hydrogen abstraction from tertiary carbon [27].
19	$\text{EL} + \ddot{\text{O}} \rightleftharpoons \text{EL3J} + \dot{\text{O}}\text{H}$	3.94×10^{-5}	2.40	1,150	Assumed to be 2 x hydrogen abstraction from tertiary carbon [27].
20	$\text{EL} + \ddot{\text{O}} \rightleftharpoons \text{EL4J} + \dot{\text{O}}\text{H}$	3.94×10^{-5}	2.40	1,150	Assumed to be 2 x hydrogen abstraction from tertiary carbon [27].
21	$\text{EL} + \ddot{\text{O}} \rightleftharpoons \text{EL6J} + \dot{\text{O}}\text{H}$	3.94×10^{-5}	2.40	1,150	Assumed to be 2 x hydrogen abstraction from tertiary carbon [27].
22	$\text{EL} + \ddot{\text{O}} \rightleftharpoons \text{EL7J} + \dot{\text{O}}\text{H}$	1.35×10^{-7}	2.03	5,136	Assumed to be 3 x hydrogen abstraction from primary carbon [27].
<i>Hydrogen Abstraction from Ethyl Levulinate by Molecular Oxygen</i>					
24	$\text{EL} + \text{O}_2 \rightleftharpoons \text{EL1J} + \text{H}\dot{\text{O}}_2$	3.00×10^{-13}	0.00	48,200	Assumed to be 3 x hydrogen abstraction from tertiary carbon [27].
25	$\text{EL} + \text{O}_2 \rightleftharpoons \text{EL3J} + \text{H}\dot{\text{O}}_2$	2.00×10^{-13}	0.00	48,200	Assumed to be 2 x hydrogen abstraction from tertiary carbon [27].
26	$\text{EL} + \text{O}_2 \rightleftharpoons \text{EL4J} + \text{H}\dot{\text{O}}_2$	2.00×10^{-13}	0.00	48,200	Assumed to be 2 x hydrogen abstraction from tertiary carbon [27].
27	$\text{EL} + \text{O}_2 \rightleftharpoons \text{EL6J} + \text{H}\dot{\text{O}}_2$	2.00×10^{-13}	0.00	48,200	Assumed to be 2 x hydrogen abstraction from tertiary carbon [27].
28	$\text{EL} + \text{O}_2 \rightleftharpoons \text{EL7J} + \text{H}\dot{\text{O}}_2$	3.00×10^{-13}	0.00	52,290	Assumed to be 3 x hydrogen abstraction from primary carbon [27].
<i>Ethyl Levulinate Alkyl and Alkoxy Radical Beta-bond Scissions</i>					
31	$\text{CH}_2\text{C}(\text{O}) + \dot{\text{C}}\text{H}_2\text{CH}_2\text{C}(\text{O})\text{OCH}_2\text{CH}_3 \rightleftharpoons \text{EL1J}$	5.00×10^{10}	0.00	6,000	Analogy to $\dot{\text{C}}\text{H}_3 + \text{CH}_2\text{CO} \rightleftharpoons \text{CH}_3\text{CO}\dot{\text{C}}\text{H}_2$ [27].
32	$\dot{\text{C}}\text{H}_3 + \text{C}(\text{O})\text{CHCH}_2\text{C}(\text{O})\text{OCH}_2\text{CH}_3 \rightleftharpoons \text{EL3J}$	1.76×10^4	2.48	6,130	Analogy to $\dot{\text{C}}\text{H}_3 + \text{CH}_2\text{CO} \rightleftharpoons \text{CH}_3\text{CO}\dot{\text{C}}\text{H}_2$ [27].
33	$\text{CH}_3\dot{\text{C}}(\text{O}) + \text{CH}_2\text{CHC}(\text{O})\text{OCH}_2\text{CH}_3 \rightleftharpoons \text{EL4J}$	1.00×10^{11}	0.00	8,420	Analogy to $\text{C}_2\text{H}_4 + \dot{\text{C}}\text{O}_2\text{CH}_2\text{CH}_3 \rightleftharpoons \dot{\text{C}}\text{H}_2\text{CH}_2\text{C}(\text{O})\text{OCH}_3$ [18, 19].
34	$\text{CH}_3\text{C}(\text{O})\text{CHCH}_2 + \dot{\text{C}}(\text{O})\text{OCH}_2\text{CH}_3 \rightleftharpoons \text{EL3J}$	1.00×10^{11}	0.00	8,420	Analogy to $\text{C}_2\text{H}_4 + \text{CH}_3\dot{\text{C}}\text{O} \rightleftharpoons \dot{\text{C}}\text{H}_2\text{CH}_2\text{COCH}_3$ [29].
35	$\text{CH}_3\text{C}(\text{O})\text{CH}_2\text{CHC}(\text{O}) + \text{C}_2\text{H}_5\dot{\text{O}} \rightleftharpoons \text{EL4J}$	2.23×10^{11}	0.00	7,800	Analogy to $\text{C}_2\text{H}_4 + \text{C}_2\text{H}_5\dot{\text{O}} \rightleftharpoons \text{C}_2\text{H}_5\text{OCH}_2\dot{\text{C}}\text{H}_2$ [29].
36	$\text{CH}_3\text{C}(\text{O})\text{CH}_2\text{CH}_2\dot{\text{C}}(\text{O}) + \text{CH}_3\text{CH}(\text{O}) \rightleftharpoons \text{EL6J}$	2.002×10^{12}	0.00	24,000	Analogy to $\text{CH}_3\text{CHO} + \text{CH}_3\text{CH}_2\dot{\text{C}}(\text{O}) \rightleftharpoons \text{CH}_3\dot{\text{C}}\text{H}_2\text{C}(\text{O})\text{OCH}_2\text{CH}_3$ [27].
37	$\text{CH}_3\text{C}(\text{O})\text{CH}_2\text{CH}_2\text{C}(\text{O})\dot{\text{O}} + \text{C}_2\text{H}_4 \rightleftharpoons \text{EL7J}$	1.32×10^4	2.48	6,130	Analogy to $\text{C}_2\text{H}_4 + \dot{\text{C}}\text{O}_2\text{CH}_2\text{CH}_3 \rightleftharpoons \dot{\text{C}}\text{H}_2\text{CH}_2\text{C}(\text{O})\text{OCH}_3$ [27].
38	$\text{CH}_2\text{C}(\text{O}) + \dot{\text{C}}\text{H}_2\text{C}(\text{O})\text{OCH}_2\text{CH}_3 \rightleftharpoons \dot{\text{C}}(\text{O})\text{CH}_2\text{CH}_2\text{C}(\text{O})\text{OCH}_2\text{CH}_3$	1.00×10^4	2.48	6,130	Analogy to $\text{C}_2\text{H}_4 + \dot{\text{C}}\text{H}_2\text{C}(\text{O})\text{OCH}_3 \rightleftharpoons \dot{\text{C}}\text{H}_2\text{C}(\text{O})\text{OCH}_3$ [29].
39	$\text{CH}_3\text{C}(\text{O})\dot{\text{C}}\text{H}_2 + \text{CH}_2\text{CO} \rightleftharpoons \text{CH}_3\text{C}(\text{O})\text{CH}_2\text{CH}_2\dot{\text{C}}(\text{O})$	1.76×10^4	2.48	6,130	Analogy to $\dot{\text{C}}\text{H}_3 + \text{CH}_2\text{C}(\text{O}) \rightleftharpoons \text{CH}_3\text{CO}\dot{\text{C}}\text{H}_2$ [27].
40	$\text{CH}_3\text{C}(\text{O})\text{CH}_2\dot{\text{C}}\text{H}_2 + \text{CO}_2 \rightleftharpoons \text{CH}_3\text{C}(\text{O})\text{CH}_2\text{CH}_2\text{C}(\text{O})\dot{\text{O}}$	1.00×10^{11}	0.00	3,936	Analogy to $\text{CO}_2 + \text{CH}_3\text{CH}_2\dot{\text{C}}\text{H}_2 \rightleftharpoons \text{CH}_3\text{CH}_2\text{CH}_2\text{C}(\text{O})\dot{\text{O}}$ [29].
41	$\text{C}_2\text{H}_4 + \text{CH}_3\dot{\text{C}}(\text{O}) \rightleftharpoons \dot{\text{C}}\text{H}_2\text{CH}_2\text{C}(\text{O})\text{CH}_3$	1.00×10^{11}	0.00	8,420	Analogy to $\text{C}_2\text{H}_4 + \text{CH}_3\dot{\text{C}}\text{O} \rightleftharpoons \dot{\text{C}}\text{H}_2\text{CH}_2\text{COCH}_3$ [29].
<i>Ethyl Levulinate Alkyl Radical Isomerisations</i>					

6	EL1J ⇌ EL3J	1.00 x10 ¹³	0.00	0.0	Assumed to be in thermodynamic equilibrium [30].
7	EL1J ⇌ EL4J	1.00 x10 ¹³	0.00	0.0	Assumed to be in thermodynamic equilibrium [30].
8	EL1J ⇌ EL6J	1.00 x10 ¹³	0.00	0.0	Assumed to be in thermodynamic equilibrium [30].
9	EL1J ⇌ EL7J	1.00 x10 ¹³	0.00	0.0	Assumed to be in thermodynamic equilibrium [30].
10	EL3J ⇌ EL4J	1.00 x10 ¹³	0.00	0.0	Assumed to be in thermodynamic equilibrium [30].
11	EL3J ⇌ EL6J	1.00 x10 ¹³	0.00	0.0	Assumed to be in thermodynamic equilibrium [30].
12	EL3J ⇌ EL7J	1.00 x10 ¹³	0.00	0.0	Assumed to be in thermodynamic equilibrium [30].
13	EL4J ⇌ EL6J	1.00 x10 ¹³	0.00	0.0	Assumed to be in thermodynamic equilibrium [30].
14	EL4J ⇌ EL7J	1.00 x10 ¹³	0.00	0.0	Assumed to be in thermodynamic equilibrium [30].
15	EL6J ⇌ EL7J	1.00 x10 ¹³	0.00	0.0	Assumed to be in thermodynamic equilibrium [30].
16	<i>Levulinic Acid Decomposition</i>				
17	CH ₃ C(O)CH ₂ CH ₂ C(O)Ö + Ḣ ⇌ CH ₃ C(O)CH ₂ CH ₂ C(O)OH	1.00 x10 ¹⁴	0.0	0.0	High pressure limit, analogy to ethyl propanoate [18, 19].
18	CH ₃ C(O)CH ₂ CHC(O)OH + Ḣ ⇌ CH ₃ C(O)CH ₂ CH ₂ C(O)OH	1.00 x10 ¹⁴	0.0	0.0	High pressure limit, analogy to ethyl propanoate [18, 19].
19	CH ₃ C(O)CHCH ₂ C(O)OH + Ḣ ⇌ CH ₃ C(O)CH ₂ CH ₂ C(O)OH	1.00 x10 ¹⁴	0.0	0.0	High pressure limit, analogy to ethyl propanoate [18, 19].
20	CH ₂ C(O)CH ₂ CH ₂ C(O)OH + Ḣ ⇌ CH ₃ C(O)CH ₂ CH ₂ C(O)OH	1.00 x10 ¹⁴	0.0	0.0	High pressure limit, analogy to ethyl propanoate [18, 19].
21	CH ₃ C(O)CH ₂ CH ₂ C(O) + ÖH ⇌ CH ₃ C(O)CH ₂ CH ₂ C(O)OH	7.00 x10 ¹³	0.0	0.0	High pressure limit, analogy to ethyl propanoate [18, 19].
22	CH ₃ C(O)CH ₂ CH ₂ C(O) + ÖH ⇌ CH ₃ C(O)CH ₂ CH ₂ C(O)OH	7.00 x10 ¹³	0.0	0.0	High pressure limit, analogy to ethyl propanoate [18, 19].
23	CH ₃ C(O)CH ₂ CH ₂ + C(O)OH ⇌ CH ₃ C(O)CH ₂ CH ₂ C(O)OH	3.00 x10 ¹³	0.0	0.0	High pressure limit, analogy to ethyl propanoate [18, 19].
24	CH ₃ C(O)CH ₂ + CH ₂ C(O)OH ⇌ CH ₃ C(O)CH ₂ CH ₂ C(O)OH	3.00 x10 ¹³	0.0	0.0	High pressure limit, analogy to ethyl propanoate [18, 19].
25	CH ₃ C(O) + CH ₂ CH ₂ C(O)OH ⇌ CH ₃ C(O)CH ₂ CH ₂ C(O)OH	3.00 x10 ¹³	0.0	0.0	High pressure limit, analogy to ethyl propanoate [18, 19].
26	CH ₃ + C(O)CH ₂ CH ₂ C(O)OH ⇌ CH ₃ C(O)CH ₂ CH ₂ C(O)OH	3.00 x10 ¹³	0.0	0.0	High pressure limit, analogy to ethyl propanoate [18, 19].
27	CH ₃ + C(O)CH ₂ CH ₂ C(O)OH ⇌ CH ₃ C(O)CH ₂ CH ₂ C(O)OH	3.00 x10 ¹³	0.0	0.0	High pressure limit, analogy to ethyl propanoate [18, 19].
28	<i>Hydrogen Abstraction from Levulinic Acid by Hydrogen Atom</i>				
29	CH ₃ C(O)CH ₂ CH ₂ C(O)OH + Ḣ ⇌ CH ₃ C(O)CH ₂ CH ₂ C(O)Ö + H ₂	2.22 x10 ⁵	2.54	6,756	Assumed to be 1 x hydrogen abstraction from primary carbon [27].
30	CH ₃ C(O)CH ₂ CH ₂ C(O)OH + Ḣ ⇌ CH ₃ C(O)CH ₂ CHC(O)OH + H ₂	1.20 x10 ⁶	2.40	2,583	Assumed to be 2 x hydrogen abstraction from tertiary carbon [27].
31	CH ₃ C(O)CH ₂ CH ₂ C(O)OH + Ḣ ⇌ CH ₃ C(O)CHCH ₂ C(O)OH + H ₂	1.20 x10 ⁶	2.40	2,583	Assumed to be 2 x hydrogen abstraction from tertiary carbon [27].
32	CH ₃ C(O)CH ₂ CH ₂ C(O)OH + Ḣ ⇌ CH ₂ C(O)CH ₂ CH ₂ C(O)OH + H ₂	1.80 x10 ⁶	2.40	2,583	Assumed to be 3 x hydrogen abstraction from tertiary carbon [27].
33	<i>Hydrogen Abstraction from Levulinic Acid by Hydrogen Atom</i>				
34	CH ₃ C(O)CH ₂ CH ₂ C(O)OH + ÖH ⇌ CH ₃ C(O)CH ₂ CH ₂ C(O)Ö + H ₂ O	1.51 x10 ⁻¹	3.65	7,154	Assumed to be 1 x hydrogen abstraction from primary carbon [27].
35	CH ₃ C(O)CH ₂ CH ₂ C(O)OH + ÖH ⇌ CH ₃ C(O)CH ₂ CHC(O)OH + H ₂ O	5.85 x10 ⁴	2.53	-1,659	Assumed to be 2 x hydrogen abstraction from tertiary carbon [27].
36	CH ₃ C(O)CH ₂ CH ₂ C(O)OH + ÖH ⇌ CH ₃ C(O)CHCH ₂ C(O)OH + H ₂ O	5.85 x10 ⁴	2.53	-1,659	Assumed to be 2 x hydrogen abstraction from tertiary carbon [27].
37	CH ₃ C(O)CH ₂ CH ₂ C(O)OH + ÖH ⇌ CH ₂ C(O)CH ₂ CH ₂ C(O)OH + H ₂ O	8.78 x10 ⁴	2.53	-1,659	Assumed to be 3 x hydrogen abstraction from tertiary carbon [27].
38	<i>Hydrogen Abstraction from Levulinic Acid by Methyl Radical</i>				
39	CH ₃ C(O)CH ₂ CH ₂ C(O)OH + CH ₃ · ⇌ CH ₃ C(O)CH ₂ CH ₂ C(O)Ö + CH ₄	1.51 x10 ⁻¹	3.65	7,154	Assumed to be 1x hydrogen abstraction from primary carbon [27].
40	CH ₃ C(O)CH ₂ CH ₂ C(O)OH + CH ₃ · ⇌ CH ₃ C(O)CH ₂ CHC(O)OH + CH ₄	1.81	3.46	4598	Assumed to be 2 x hydrogen abstraction from tertiary carbon [27].
41	CH ₃ C(O)CH ₂ CH ₂ C(O)OH + CH ₃ · ⇌ CH ₃ C(O)CHCH ₂ C(O)OH + CH ₄	1.81	3.46	4598	Assumed to be 2 x hydrogen abstraction from tertiary carbon [27].
42	CH ₃ C(O)CH ₂ CH ₂ C(O)OH + CH ₃ · ⇌ CH ₂ C(O)CH ₂ CH ₂ C(O)OH + CH ₄	2.71	3.46	4598	Assumed to be 3 x hydrogen abstraction from tertiary carbon [27].
43	<i>Hydrogen Abstraction from Levulinic Acid by Methoxy Radical</i>				

6	$\text{CH}_3\text{C}(\text{O})\dot{\text{C}}\text{HCH}_2\text{C}(\text{O})\text{OH} \rightleftharpoons \dot{\text{C}}\text{H}_2\text{C}(\text{O})\text{CH}_2\text{CH}_2\text{C}(\text{O})\text{OH}$	1.00×10^{13}	0.00	0.0	Assumed to be in thermodynamic equilibrium [30].
7	<i>Ethyl Propanoate Submodel</i>				
8	$\dot{\text{C}}\text{H}_2\text{CH}_2\text{C}(\text{O})\text{OCH}_2\text{CH}_3 \rightleftharpoons \text{C}_2\text{H}_4 + \text{CH}_3\text{CH}_2\text{O}\dot{\text{C}}(\text{O})$	4.638×10^{18}	-1.28	53,860	Adopted from ethyl propanoate [18, 19].
9	$\text{CH}_3\text{CH}_2\text{O}\dot{\text{C}}(\text{O}) + \text{M} \rightleftharpoons \text{CH}_3\text{CH}_2\dot{\text{O}} + \text{CO} + \text{M}$	1.000×10^{13}	0.00	10,000	Adopted from ethyl propanoate [18, 19].
10	$\text{CH}_3\text{CH}_2\text{O}\dot{\text{C}}(\text{O}) + \text{M} \rightleftharpoons \text{CH}_3\dot{\text{C}}\text{H}_2 + \text{CO}_2 + \text{M}$	5.059×10^{14}	0.17	25,520	Adopted from ethyl propanoate [18, 19].
11	$\text{CH}_3\text{CH}_2\text{C}(\text{O})\text{O}\dot{\text{C}}\text{H}_2 \rightleftharpoons \text{CH}_2\text{O} + \text{CH}_3\text{CH}_2\dot{\text{C}}(\text{O})$	9.364×10^{19}	-1.88	56,420	Adopted from methyl butanoate [18, 19].
12	$\text{CH}_2\text{CHC}(\text{O})\text{O}\dot{\text{C}}\text{H}_2 \rightleftharpoons \text{CH}_2\text{O} + \text{CH}_2\text{CH}\dot{\text{C}}(\text{O})$	7.949×10^{20}	-1.82	44,530	Adopted from methyl butanoate [18, 19].
13	$\dot{\text{C}}\text{H}_2\text{C}(\text{O})\text{OCH}_2\text{CH}_3 \rightleftharpoons \text{CH}_2\text{CO} + \text{CH}_3\text{CH}_2\dot{\text{O}}$	1.805×10^{16}	-0.56	20,170	Adopted from ethyl propanoate [18, 19].
14	$\text{CO} + \dot{\text{C}}\text{H}_2\text{CH}_2\text{C}(\text{O})\text{OH} + \text{M} \rightleftharpoons \dot{\text{C}}(\text{O})\text{CH}_2\text{CH}_2\text{C}(\text{O})\text{OH} + \text{M}$	8.827×10^{15}	-0.67	35,550	Adopted from ethyl propanoate [18, 19].
15	$\dot{\text{C}}\text{H}_2\text{CH}_2\text{C}(\text{O})\text{OH} \rightleftharpoons \text{C}_2\text{H}_4 + \dot{\text{C}}(\text{O})\text{OH}$	1.510×10^{11}	0.00	4,810	Adopted from ethyl propanoate [18, 19].
16	$\dot{\text{C}}\text{H}_2\text{C}(\text{O})\text{OH} \rightleftharpoons \text{CH}_2\text{CO} + \dot{\text{O}}\text{H}$	2.418×10^{23}	-2.82	36,410	Adopted from ethyl propanoate [18, 19].
17	<i>Acrylic Acid Submodel</i>				
18	$\text{CH}_2\text{CHC}(\text{O})\text{OH} \rightleftharpoons \text{CH}_2\dot{\text{C}}\text{H} + \dot{\text{C}}(\text{O})\text{OH}$	3.752×10^{21}	-1.89	112,900	Adopted from ethyl propanoate [18, 19].
19	$\text{CH}_2\text{CHC}(\text{O})\text{OH} \rightleftharpoons \text{CH}_2\text{CH}\dot{\text{C}}(\text{O}) + \dot{\text{O}}\text{H}$	5.206×10^{20}	-1.16	100,900	Adopted from ethyl propanoate [18, 19].
20	$\text{CH}_2\text{CH}\dot{\text{C}}(\text{O}) + \dot{\text{O}}\text{H} \rightleftharpoons \text{C}_2\text{H}_4 + \text{CO}_2$	1.000×10^{12}	0.00	0	Adopted from ethyl propanoate [18, 19].
21	$\text{CH}_2\text{CH}\dot{\text{C}}(\text{O}) + \text{H}\dot{\text{O}}_2 \rightleftharpoons \text{CH}_2\dot{\text{C}}\text{H} + \text{CO}_2 + \dot{\text{O}}\text{H}$	6.030×10^9	0.00	7,949	Adopted from ethyl propanoate [18, 19].
22	$\text{CH}_2\text{CH}\dot{\text{C}}(\text{O}) + \text{CH}_3\dot{\text{O}}_2 \rightleftharpoons \text{CH}_2\dot{\text{C}}\text{H} + \text{CO}_2 + \text{CH}_3\dot{\text{O}}$	3.970×10^{11}	0.00	17,050	Adopted from ethyl propanoate [18, 19].
23	$\dot{\text{C}}(\text{O})\text{OH} + \text{M} \rightleftharpoons \text{CO} + \dot{\text{O}}\text{H} + \text{M}$	1.186×10^{14}	0.13	36,460	Adopted from ethyl propanoate [18, 19].
24	$\dot{\text{C}}(\text{O})\text{OH} + \text{M} \rightleftharpoons \text{CO}_2 + \text{H} + \text{M}$	8.220×10^{11}	0.41	35,340	Adopted from ethyl propanoate [18, 19].

Table 4. Reaction pathways, estimated rate constants and sources for the reactions of the ethyl levulinate sub model. Rate coefficients are in the form $k = A T^n \exp(-E_a/RT)$, cm³/mole/s. Activation energies are in calories/mol.

4.3 Submodels, Small Species Chemistry and Model Calculations

A purpose of the kinetic model is to aid in the comprehension of the use of this potential biofuel when blended with conventional fuels, such as gasoline. To allow for this pursuit, the ethyl levulinate chemistry is added to the primary/toluene reference fuel kinetic model of Mehl et al. [31], therefore assuming the validity of that state of the art construct.

The modelling computations in this study are carried out using the closed homogeneous (senkin) subroutine of ChemkinPro. The fundamental modelling assumptions used in comparing the purely chemical kinetic calculations with experiments are as follows; shock tube simulations are zero dimensional and begin at the onset of the reflected shock period assuming constant volume and homogeneous adiabatic conditions behind the reflected shock wave and consistent with the experimentally observed pressure profiles. The reflected shock pressure and temperature are inputted as the initial pressure and temperature, respectively. The simulated ignition delay time is defined as per the experiment. RCM simulations, are similar, but use the volume history approach to describe the heat losses in the post compression period. The kinetic model, all pertinent experimental data, including volume histories are available from the authors upon request.

5. Results and Discussion

5.1 Ethyl Levulinate Ignition Delay

The ignition delay data for ethyl levulinate is compared to model simulations in Figure 4. The shock tube data, 1100-1400 K, is characterised by the normal Arrhenius like temperature dependence, and increase in reactivity with increased oxygen concentration. The RCM data behaves similarly, and is seemingly consistent with the shock tube data, showing longer ignition delays due to the dynamic temperature characteristic of that device, resulting in an apparent change in activation energy. The truncated temperature range in which ethyl levulinate is reactive is notable, showing no ignition at temperatures lower than ~1040 K. The kinetic model reproduces the shock tube measured reactivity rather closely, to with a maximum deviation of $\pm 30\%$, accurately capturing the reactivity dependence

1 on temperature and oxygen concentration. Figure 4 shows that the modelling protocol reproduces the
2 RCM ignition times to a lesser fidelity. Considering the weak energy density of the mixtures studied
3 and the dynamic temperature environment of the RCM, we believe that the physical models assumed
4 in the simulations more adequately approximate the conditions generated by the shock tube, than
5 those of the RCM. It is known that low energy density, low pressure compressed states show a greater
6 propensity to form cool boundary layers in the RCM [15], exacerbating undesired fluid dynamic
7 perturbations to the intended adiabatic core gas. In Figure 4, the constant volume model calculations
8 are extended to the temperatures of the RCM measurements and provide an easier reference for
9 gauging the reactivity of ethyl levulinate at low temperatures. The model shows ethyl levulinate to
10 exhibit Arrhenius type dependence across the studied temperature range, though not shown in Figure
11 4 for clarity, ceasing to ignite at time scales lower than 500 ms between 800-700 K. We emphasize
12 that the model inputs have not been adjusted from the “best knowledge” estimates described above, to
13 better reproduce one data set over the other. This being the case, the modelling methodology
14 demonstrates the applicability of the functionality concept in kinetic modelling, and the accuracy of
15 the underpinning thermochemistry study and prior kinetic modelling studies of other embodiments of
16 the functionalities that comprise ethyl levulinate, e.g. [4, 5, 17-20, 22-26, 31].
17
18
19
20
21
22
23
24
25
26
27
28
29
30
31
32
33
34
35
36
37
38
39
40
41
42
43
44
45
46
47
48
49
50
51
52
53
54
55
56
57
58
59
60
61
62
63
64
65

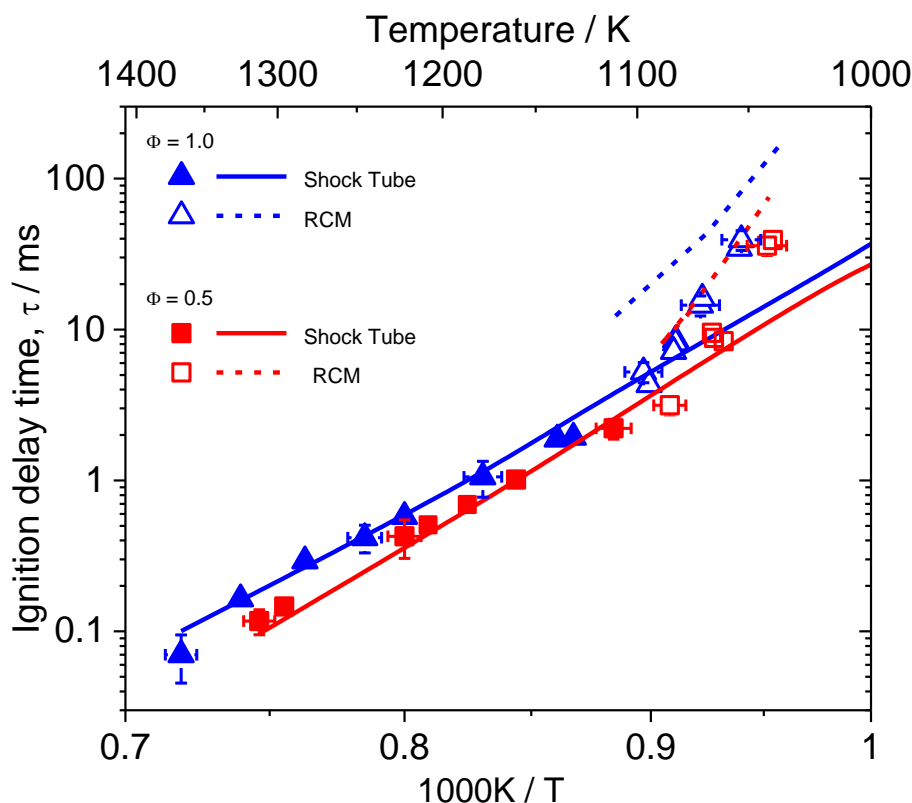


Figure 4. Shock tube and rapid compression machine ignition delay times for 0.5% ethyl levulinate, ϕ 1.0 and ϕ 0.5, at ~ 10 atm.

5.2 Kinetic Model Analysis

Chemical flux and sensitivity analyses of a 0.5% ethyl levulinate oxidation at 1250 K and 10.4 atm for the stoichiometric mixture are presented in Figure 5 and 6 respectively, as representative of the range of test conditions studied. The flux analysis paints a simple picture of ethyl levulinate oxidation under induction conditions, showing that almost 96% of the ethyl levulinate fuel decomposes to levulinic acid and ethylene as molecular products. Approximately 2.6% of the fuel undergoes simple fission of the weaker C–C and C–O bonds, leaving only minute quantities of ethyl levulinate to be consumed by hydrogen abstraction reactions. This analysis would therefore indicate that the uncertainty in the prescription of rate constants to the unusually weak C–H bonds, is not an especially corrupting uncertainty to the model overall. This simplistic oxidation behavior is in notable contrast to what has been reported many times for alkanes and other oxygenates, where hydrogen abstraction and alkyl radical beta bond scission are commanding processes. The simplicity of the ethyl

levulinate oxidation mechanism is thus notable, but completely consistent with the suggestions of other workers concerning other ethyl esters [18, 19, 24-26] and indeed basically verifying the assumptions made by Tian et al in attempting to explain the engine reactivity of ethyl levuliate.

1
2
3
4
5
6
7
8
9
10
11
12
13
14
15
16
17
18
19
20
21
22
23
24
25
26
27
28
29
30
31
32
33
34
35
36
37
38
39
40
41
42
43
44
45
46
47
48
49
50
51
52
53
54
55
56
57
58
59
60
61
62
63
64
65

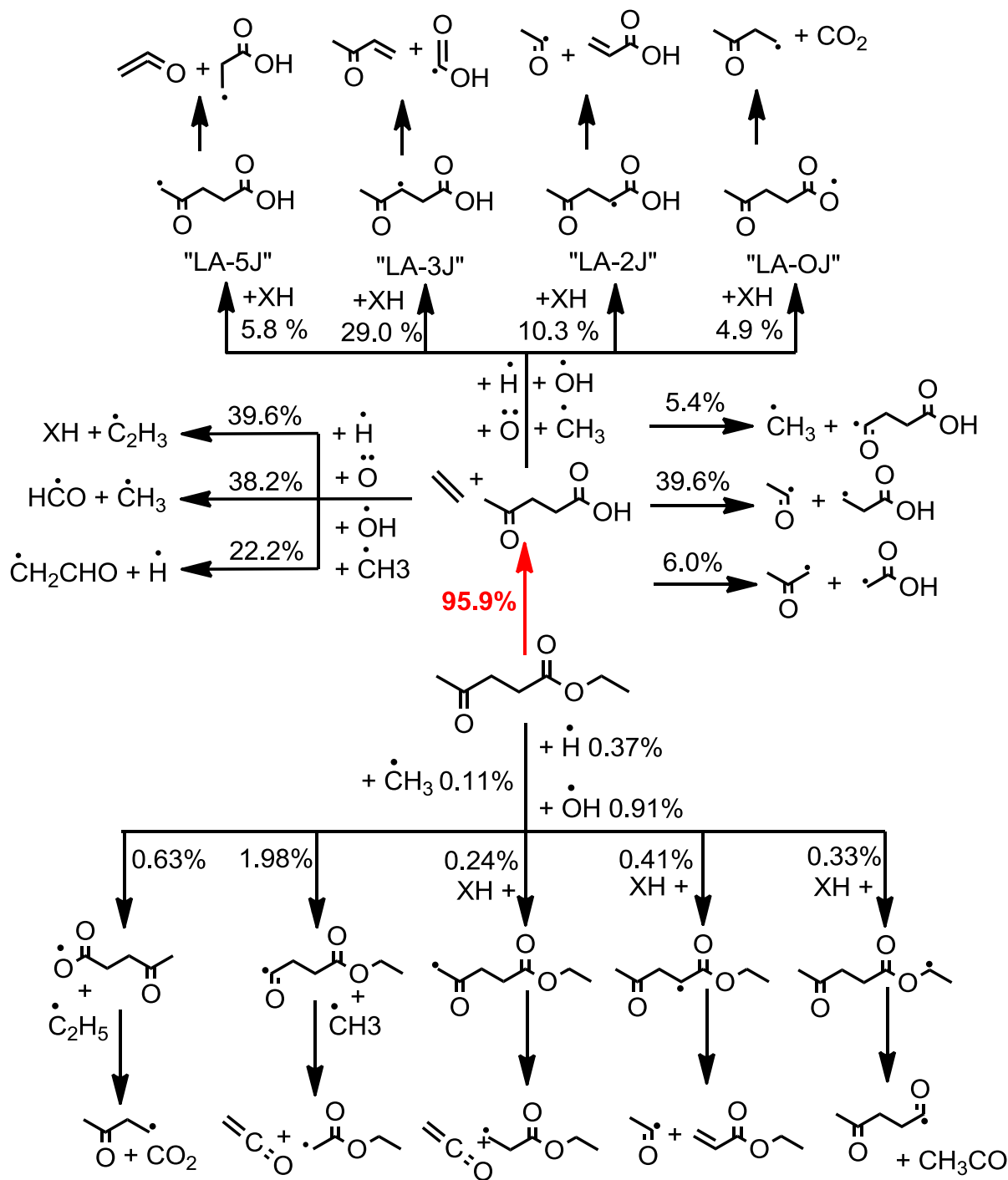


Figure 5. Reacting flux analysis at the point of 50% ethyl levulinate consumption for shock tube simulation of 0.5% fuel, ϕ 1.0 at 10.4 atm and 1250 K.

1
2
3
4
5
6
7
8
9
10
11
12
13
14
15
16
17
18
19
20
21
22
23
24
25
26
27
28
29
30
31
32
33
34
35
36
37
38
39
40
41
42
43
44
45
46
47
48
49
50
51
52
53
54
55
56
57
58
59
60
61
62
63
64
65

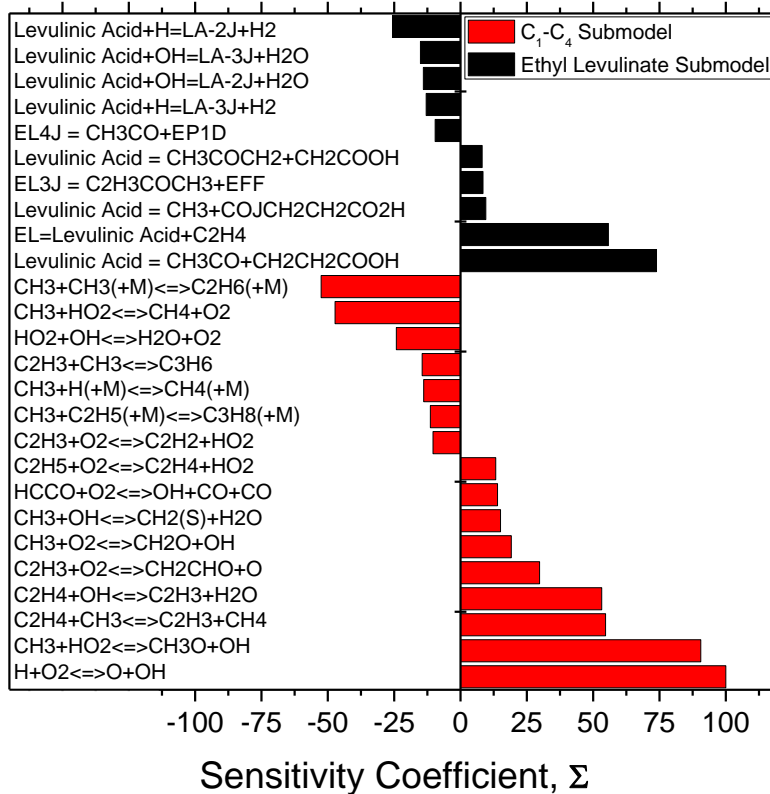


Figure 6. Sensitivity analysis to ΔT in ethyl levulinate shock tube ignition delay simulation for 0.5% fuel, ϕ 1.0 at 10.4 atm and 1250 K. “LA-“X”J” designates levulinic acid radicals per Figure 5.

Figure 6 shows a sensitivity analysis of the reactions effecting ΔT , the analyses is divided into reactions of the ethyl levulinate submodel and to reactions of the small species chemistry. A positive value indicates that a reaction increases the temperature of the system, leading to ignition. As expected, the most sensitive reaction at this 1250 K condition is the $H + O_2 \rightleftharpoons O + OH$, the magnitude of all sensitivity coefficients have been normalized to this reference. An arbitrary threshold of 10% of this value has been imposed for a reaction to be included in Figure 6. The analysis shows the ethyl levulinate submodel to be dominated by the chemistry accounting for levulinic acid production and consumption. The ethyl levulinate elimination reaction is the fourth most sensitive reaction in the system, with the further unimolecular decomposition of levulinic acid to produce two radicals the most reactivity enhancing reaction in the ethyl levulinate submodel. For this reason, the occurrence of

1 hydrogen abstraction reactions that consume either ethyl levulinate, or levulinic acid, produce a
2 negative effect on the reactivity of the system. Examination of the role of the chemistry of the
3 submodel reveals the influence of ethylene, the co-product to levulinic acid formation. The vinyl
4 radical is formed by hydrogen abstraction from ethylene and subsequently consumed by addition of
5 O₂, Figure 6. Reactions which produce the vinyl radical show a strong positive influence on the
6 reaction rate, as it is predominantly consumed by reaction with O₂ to form radical chain branching
7 products of CH₂CHO + O. From the above analysis, the importance of the levulinic acid oxidation
8 mechanism to the combustion of ethyl levulinate is clearly apparent. It should be noted that levulinic
9 acid combustion is entirely unstudied. If ethyl levulinate does find eventual commercial use as a
10 transportation fuel component, a more detailed understanding of its combustion mechanism may be
11 required, at that time the levulinic acid submodel may be worthy of dedicated attention.
12
13
14
15
16
17
18
19
20
21
22
23
24
25

26 **5.3 Ethyl Levulinate Octane Number Calculation**

27
28 With an accurate kinetic model for ethyl levulinate and ternary reference fuel combustion, the
29 research octane number (RON) and the motor octane number (MON) of ethyl levulinate can be
30 estimated using the relationship proposed by Singh et al. [32], which correlates model calculated
31 ignition delay time to the RON ("IDT to RON") and to the MON ("IDT to MON") of the fuel. Singh
32 et al. developed the two models using a double exponential equation to describe the relationship
33 between the ignition delay time and the octane number of the form:
34
35
36
37
38
39
40
41

$$42 \quad xON = a + (b \cdot \exp^{-IDT/c}) + (d \cdot \exp^{-IDT/e})$$

43
44 Where xON can either be RON or MON, IDT refers to the ignition delay time and a , b , c , d and e are
45 the model parameters which are determined by the minimization of errors between the measured and
46 predicted (simulated) values.
47
48
49
50

51 The ignition delay times used by Singh et al. to develop the IDT-to-RON and IDT-to-MON
52 models were calculated using a different chemical kinetic model than the one used in this. Thus, for
53 better accuracy, the parameters ($a - e$) derived by Singh et al., for both the IDT-to-RON and IDT-to-
54 MON models, were re-estimated using ignition delay times calculated by the model constructed in
55
56
57
58
59
60

1 this study. For the re-estimation of the model parameters in the IDT-to-RON model, ignition delay
2 times were calculated for the reference fuel blends, outlined in Table S1, at a temperature of 750 K, a
3
4 pressure of 25 bar and equivalence ratio of 1, and for the IDT-to-MON model at a temperature of 825
5
6 K, pressure of 25 bar and equivalence ratio of 1, as Singh et al. noted these conditions resulted in the
7
8 best correlation between the ignition delay time and the respective octane number. Values calculated
9
10 for the parameters a to e for both IDT-to-RON and IDT-to-MON models can be seen in Table 5 and
11
12 offer good agreement between the model predicted octane numbers and the experimentally calculated
13
14 octane numbers, as seen in Figure 7, with the IDT-to-RON model having an R^2 value of 0.9943 and
15
16 the IDT-to-MON model having an R^2 value of 0.9882. Here it is necessary to note, that the models
17
18 indicated by Table S1 in Supporting Information are different in detail to those proposed by Singh et
19
20 al. The reason for this is due to slight differences in the ignition delay computed by the kinetic model
21
22 constructed in this study, to those computed by the kinetic model of Singh et al. for the same mixture
23
24 composition.
25
26
27
28
29
30

31 The ignition delay time for ethyl levulinate at a temperature of 750 K, a pressure of 25 bar
32
33 and equivalence ratio 1 is calculated to be 0.263 s. Using the IDT-to-RON model derived in this
34
35 study, the RON for ethyl levulinate is estimated to be 97.7. The ignition delay time for ethyl
36
37 levulinate at a temperature of 825 K, a pressure of 25 bar and equivalence ratio of 1 is calculated to be
38
39 0.0498 s. Using the IDT-to-MON model derived in this study, the MON for ethyl levulinate is
40
41 estimated to be 93. This analysis indicates that from a pre-vaporised kinetic stand point, ethyl
42
43 levulinate is much more suitable as a spark ignition, gasoline type fuel than as a diesel fuel
44
45 component, as has been suggested by previous studies.
46
47
48
49
50

51 From ignition quality tests, Tian et al. [14] found that ethyl levulinate had a superior anti-
52
53 knock quality than EURO 95 gasoline (RON = 95) and iso-octane (RON 100). Thus, from their
54
55 results one would expect ethyl levulinate to have a RON greater than 100. The predicted ethyl
56
57 Levulinate RON in this work is 97.7, it must be noted that the RON and MON estimation technique
58
59
60
61
62
63
64
65

employed in this study are limited to the extremes of the RON and MON ranges studied by Singh et al, i.e. <100 octane numbers. The estimates of ethyl levulinate octane numbers quoted above are therefore to be more accurately defined as RON ≥ 97.7 and MON ≥ 93 .

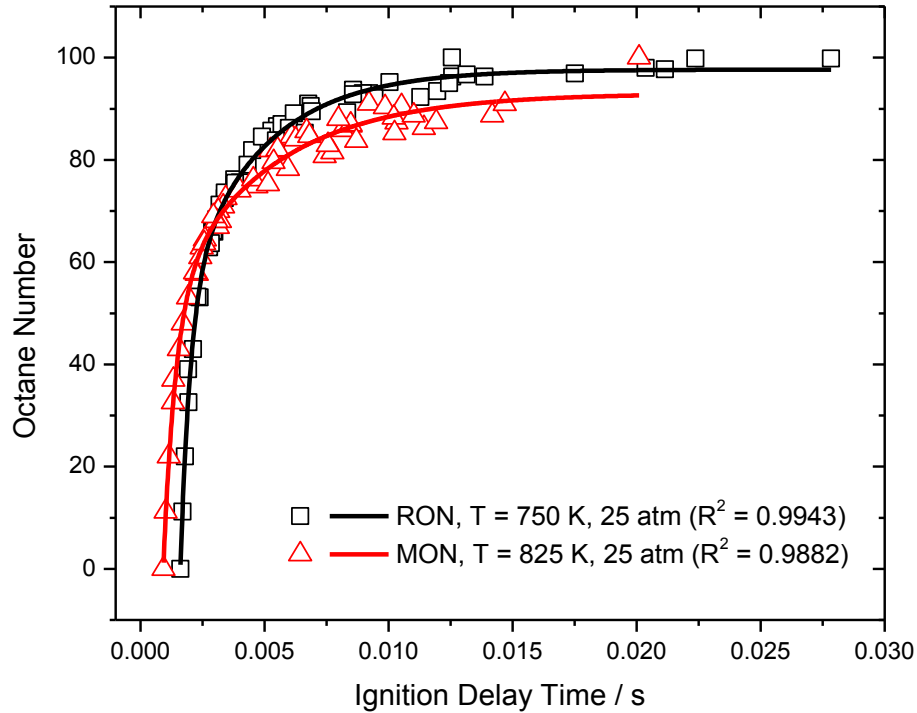


Figure 7. Measured Research (RON) and Motored Octane Numbers (MON) of Singh et al. [32] (symbols) vs calculated ignition delay times from this study (lines), for the reference fuels described in Table S1 (symbols). Ignition delay times were calculated at a pressure of 25 bar, an equivalence ratio of 1 and a temperature of 750 K and 825 K to represent the RON and MON conditions respectively.

Parameter	Model	
	"IDT to RON"	"IDT to MON"
A	$9.77 \times 10^{+1}$	$9.30 \times 10^{+1}$
B	$-2.58 \times 10^{+3}$	$-3.24 \times 10^{+2}$
C	4.15×10^{-4}	5.05×10^{-4}
D	$-7.31 \times 10^{+1}$	$-5.03 \times 10^{+1}$
E	3.16×10^{-3}	4.17×10^{-3}

Table 5. Estimated model parameters for the IDT-to-RON and IDT-to-MON models.

5. Conclusions

The gas phase combustion kinetics of the proposed lignocellulosic biofuel, ethyl levulinate (EL), have been studied. Shock tube and rapid compression machine measured ignition delays show the molecule to exhibit a truncated range of reactivity, igniting at temperatures above ~ 1040 K at 10 atm.

A detailed kinetic model for ethyl levulinate combustion is proposed substantially based on these calculations and stands ready to be used for the consideration of ethyl levulinate with gasoline reference fuels in combustion simulations. The model suggests that ethyl levulinate oxidation induction chemistry to be dominated by the ethyl ester, rather than the ketone, functionality of the fuel structure. As is characteristic of ethyl esters, ethyl levulinate predominantly decomposes to form an acid, in levulinic acid, and ethylene. Reacting flux and sensitivity analysis of the model show the oxidation chemistry of these species to dominate the temporal occurrence of ethyl levulinate ignition under the conditions tested. Calculations performed with the kinetic model estimate the RON and MON of ethyl levulinate to be ≥ 97.7 and ≥ 93 , respectively. This suggests that ethyl levulinate would be best suited as a gasoline fuel component rather than a diesel fuel component as prevalent in the literature, indeed it may be considered to be useful as an octane booster.

Acknowledgements

Research (University of Limerick, Trinity College Dublin & KAUST) reported in this publication was carried out under the Future Fuels project supported by the Competitive Center Funding (CCF) program at King Abdullah University of Science and Technology (KAUST). Research conducted at National University of Ireland, Galway and Trinity College Dublin was supported by Science Foundation Ireland. Computational resources were provided by the Irish Centre for High-End Computing, ICHEC.

Supplementary Materials

Supplementary material associated with this article can be found, in the online version, at doi:xxx.

References

- [1] M. Mascal, E.B. Nikitin, High-yield conversion of plant biomass into the key value-added feedstocks 5-(hydroxymethyl)furfural, levulinic acid, and levulinic esters via 5-(chloromethyl)furfural, *Green Chemistry* 12 (2010) 370-373.
- [2] T. Flannelly, S. Dooley, J.J. Leahy, Reaction Pathway Analysis of Ethyl Levulinate and 5-Ethoxymethylfurfural from d-Fructose Acid Hydrolysis in Ethanol, *Energy & Fuels* 29 (2015) 7554-7565.
- [3] M.K. Ghosh, S. Dooley, Accurate Thermochemistry for Oxygenate Hydrocarbons, A Case Study (In Preparation). Supplementary Materials Provided for Review.
- [4] A.M. El-Nahas, M.V. Navarro, J.M. Simmie, J.W. Bozzelli, H.J. Curran, S. Dooley, W. Metcalfe, Enthalpies of Formation, Bond Dissociation Energies and Reaction Paths for the Decomposition of Model Biofuels: Ethyl Propanoate and Methyl Butanoate, *The Journal of Physical Chemistry A* 111 (2007) 3727-3739.
- [5] J.M. Hudzik, J.W. Bozzelli, Thermochemistry and bond dissociation energies of ketones, *J Phys Chem A* 116 (2012) 5707-5722.
- [6] T. Lei, Z. Wang, Y. Li, Z. Li, X. He, J. Zhu, Performance of a Diesel Engine with Ethyl Levulinate-Diesel Blends: A Study using Grey Relational Analysis, 2013.
- [7] E. Koivisto, N. Ladommatos, M. Gold, Compression Ignition and Exhaust Gas Emissions of Fuel Molecules Which Can Be Produced from Lignocellulosic Biomass: Levulinates, Valeric Esters, and Ketones, *Energy & Fuels* 29 (2015) 5875-5884.
- [8] B.C. Windom, T.M. Lovestead, M. Mascal, E.B. Nikitin, T.J. Bruno, Advanced distillation curve analysis on ethyl levulinate as a diesel fuel oxygenate and a hybrid biodiesel fuel, *Energy & Fuels* 25 (2011) 1878-1890.
- [9] M.J. Murphy, J.D. Taylor, R.L. McCormick, Compendium of experimental cetane number data, National Renewable Energy Laboratory, NREL/SR-540-36805, (2004).
- [10] E. Christensen, A. Williams, S. Paul, S. Burton, R.L. McCormick, Properties and Performance of Levulinate Esters as Diesel Blend Components, *Energy & Fuels* 25 (2011) 5422-5428.

- 1
2
3
4
5
6
7
8
9
10
11
12
13
14
15
16
17
18
19
20
21
22
23
24
25
26
27
28
29
30
31
32
33
34
35
36
37
38
39
40
41
42
43
44
45
46
47
48
49
50
51
52
53
54
55
56
57
58
59
60
61
62
63
64
65
- [11] M.A. Lake, S.W. Burton, Diesel fuel compositions containing levulinate ester, Google Patents, 2010.
- [12] H. Joshi, B.R. Moser, J. Toler, W.F. Smith, T. Walker, Ethyl levulinate: A potential bio-based diluent for biodiesel which improves cold flow properties, *Biomass and bioenergy* 35 (2011) 3262-3266.
- [13] E. Christensen, J. Yanowitz, M. Ratcliff, R.L. McCormick, Renewable Oxygenate Blending Effects on Gasoline Properties, *Energy & Fuels* 25 (2011) 4723-4733.
- [14] M. Tian, R.L. McCormick, J. Luecke, E. de Jong, J.C. van der Waal, G.P.M. van Klink, M.D. Boot, Anti-knock quality of sugar derived levulinic esters and cyclic ethers, *Fuel* 202 (2017) 414-425.
- [15] J. Würmel, J.M. Simmie, CFD studies of a twin-piston rapid compression machine, *Combustion and Flame* 141 (2005) 417-430.
- [16] A.S. AlRamadan, J. Badra, T. Javed, M. Al-Abbad, N. Bokhumseen, P. Gaillard, H. Babiker, A. Farooq, S.M. Sarathy, Mixed butanols addition to gasoline surrogates: Shock tube ignition delay time measurements and chemical kinetic modeling, *Combustion and Flame* 162 (2015) 3971-3979.
- [17] Z. Serinyel, N. Chaumeix, G. Black, J.M. Simmie, H.J. Curran, Experimental and Chemical Kinetic Modeling Study of 3-Pentanone Oxidation, *The Journal of Physical Chemistry A* 114 (2010) 12176-12186.
- [18] W.K. Metcalfe, S. Dooley, H.J. Curran, J.M. Simmie, A.M. El-Nahas, M.V. Navarro, Experimental and Modeling Study of C₅H₁₀O₂ Ethyl and Methyl Esters, *The Journal of Physical Chemistry A* 111 (2007) 4001-4014.
- [19] W.K. Metcalfe, C. Togbé, P. Dagaut, H.J. Curran, J.M. Simmie, A jet-stirred reactor and kinetic modeling study of ethyl propanoate oxidation, *Combustion and Flame* 156 (2009) 250-260.
- [20] E.R. Ritter, J.W. Bozzelli, THERM: Thermodynamic property estimation for gas phase radicals and molecules, *International Journal of Chemical Kinetics* 23 (1991) 767-778.
- [21] H.J. Curran, P. Gaffuri, W.J. Pitz, C.K. Westbrook, A Comprehensive Modeling Study of n-Heptane Oxidation, *Combustion and Flame* 114 (1998) 149-177.

- 1
2 [22] H.J. Curran, P. Gaffuri, W.J. Pitz, C.K. Westbrook, A comprehensive modeling study of iso-
3 octane oxidation, *Combustion and Flame* 129 (2002) 253-280.
- 4 [23] A.T. Blades, P.W. Gilderson, KINETICS OF THE THERMAL DECOMPOSITION OF ETHYL
5 PROPIONATE, *Can J Chem* 38 (1960) 1412-1415.
- 6
7
8 [24] C.K. Westbrook, W.J. Pitz, P.R. Westmoreland, F.L. Dryer, M. Chaos, P. Osswald, K. Kohse-
9 H \ddot{o} inghaus, T.A. Cool, J. Wang, B. Yang, N. Hansen, T. Kasper, A detailed chemical kinetic reaction
10 mechanism for oxidation of four small alkyl esters in laminar premixed flames, *Proceedings of the*
11 *Combustion Institute* 32 (2009) 221-228.
- 12
13 [25] A. Farooq, D.F. Davidson, R.K. Hanson, C.K. Westbrook, A comparative study of the chemical
14 kinetics of methyl and ethyl propanoate, *Fuel* 134 (2014) 26-38.
- 15
16 [26] W. Ren, R. Mitchell Spearrin, D.F. Davidson, R.K. Hanson, Experimental and Modeling Study
17 of the Thermal Decomposition of C3–C5 Ethyl Esters Behind Reflected Shock Waves, *The Journal of*
18 *Physical Chemistry A* 118 (2014) 1785-1798.
- 19
20 [27] A. mech., <http://www.nuigalway.ie/c3/aramco2/frontmatter.html>.
- 21
22 [28] J.P. Orme, H.J. Curran, J.M. Simmie, Experimental and Modeling Study of Methyl Cyclohexane
23 Pyrolysis and Oxidation, *The Journal of Physical Chemistry A* 110 (2006) 114-131.
- 24
25 [29] S. Dooley, H.J. Curran, J.M. Simmie, Autoignition measurements and a validated kinetic model
26 for the biodiesel surrogate, methyl butanoate, *Combustion and Flame* 153 (2008) 2-32.
- 27
28 [30] M. Chaos, A. Kazakov, Z. Zhao, F.L. Dryer, A high-temperature chemical kinetic model for
29 primary reference fuels, *International Journal of Chemical Kinetics* 39 (2007) 399-414.
- 30
31 [31] M. Mehl, W.J. Pitz, C.K. Westbrook, H.J. Curran, Kinetic modeling of gasoline surrogate
32 components and mixtures under engine conditions, *Proceedings of the Combustion Institute* 33 (2011)
33 193-200.
- 34
35 [32] E. Singh, J. Badra, M. Mehl, S.M. Sarathy, Chemical Kinetic Insights into the Octane Number
36 and Octane Sensitivity of Gasoline Surrogate Mixtures, *Energy & Fuels* 31 (2017) 1945-1960.
- 37
38
39
40
41
42
43
44
45
46
47
48
49
50
51
52
53
54
55
56
57
58
59
60
61
62
63
64
65

Supplementary Material

[Click here to download Supplementary Material: Ghosh_Ethyl levulinate combustion kinetics_Nov_2017_to _CnF _SI.DOCX](#)

Additional Material

[Click here to download Additional Material: Ghosh_Ethyl levulinate combustion kinetics_SCI for Review Only.DOCX](#) [References](#)